ACS OMEGA

Open Access

http://pubs.acs.org/journal/acsodf

Review

Investigations of Li-Ion Battery Thermal Management Systems Based on Heat Pipes: A Review

Hanming Wu, Ming Niu, Yuankai Shao, Maoxuan Wang, Menghan Li, Xin Liu,* and Zhenguo Li*

Cite This: *ACS Omega* 2024, 9, 97−116

Read Online

ACCESS | Metrics & More | Article Recommendations

ABSTRACT: With increasing concerns about carbon emissions and the resulting climate impacts, Li-ion batteries have become one of the most attractive energy sources, especially in the transportation sector. For Li-ion batteries, an effective thermal management system is essential to ensure high-efficiency operation, avoid capacity degradation, and eliminate safety issues. Thermal management systems based on heat pipes can achieve excellent cooling performance in limited space and thus have been widely used for the temperature control of Li-ion batteries. In this paper, the thermal management systems of Li-ion batteries based on four types of heat pipes, i.e., flat single-channel heat pipes, oscillating heat pipes, flexible heat pipes, and microchannel heat pipes, are comprehensively reviewed based on the studies in the past 20 years. The effects of different influencing factors on the cooling performance and thermal runaway behavior of Li-ion batteries are thoroughly discussed in order to provide an in-depth understanding for researchers and engineers. It is concluded that for all types of thermal management systems based on heat pipes, water spray cooling could achieve better cooling performance than forced air cooling and water bath cooling, while its energy consumption is obviously smaller than forced air cooling. For thermal management systems based on oscillating heat pipes, improved heat transfer characteristics could be achieved by increasing the number of turns, using a relatively larger inner hydraulic diameter and using a length ratio between the evaporator and condenser higher than 1.0. Heat pipes fabricated by flexible materials suffer from permeation of noncondensable gases from ambient and leakage of working fluid. These issues could be partly resolved by adding thermal vias filled with metallic materials and covering the sealing part with indium coating or designing a multilayered structure with metallic materials in it. Moreover, the limitations and future trends of Li-ion battery thermal management systems based on heat pipes are presented. It is pointed out that the thermal runaway behavior and heating performance of battery thermal management systems based on heat pipes should be further elaborated. The analysis of this paper could provide valuable support for future investigations on Li-ion battery thermal management systems based on heat pipes; it could also guide the choice and design of Li-ion battery thermal management systems based on heat pipes in commercial use.

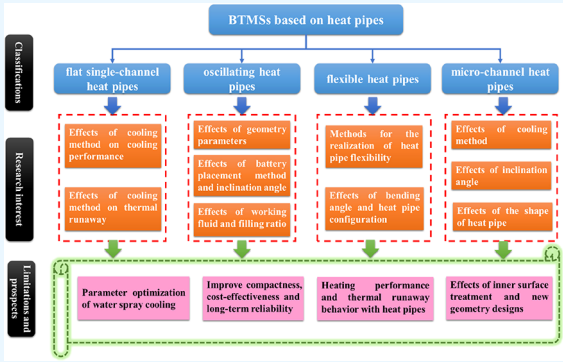

1. INTRODUCTION

From 1980 to 2023, globally averaged mole fraction of CO_2 has increased from 338.9 to 416.8 ppm over marine surface sites. Meanwhile, the averaged annual growth of CO_2 has been more than 2.0 ppm in the recent ten years,[1] which increases the tendency of global warming and may lead to more frequent occurrence of natural disasters. According to statistics, more than 20% of the global CO_2 emissions is contributed by the transportation sector.[2] Due to the increasing requirements of carbon emission reduction, vehicles have been continuously electrified in recent decades. For electrified vehicles, including electric vehicles (EV) and hybrid electric vehicles (HEV), lithium-ion (Li-ion) batteries are superior to other batteries due to their advantages in energy density, reliability, good discharging characteristics, and high voltage. Thus, Li-ion batteries are the most widely used energy source in electrified vehicles.[3,4]

The charging and discharging processes of Li-ion batteries are accompanied by heat production. The total heat production consists of the reversible heat generated caused by electrochemical reactions, together with the change of entropy, along with the irreversible heat caused by Ohmic resistance, polarization resistance, and side reactions.[5−8] Thereby, the temperature of Li-ion batteries would increase gradually if no heat removal method was employed. As investigated, the most adaptive temperature range for the

Received: October 14, 2023
Revised: November 25, 2023
Accepted: November 28, 2023
Published: December 26, 2023

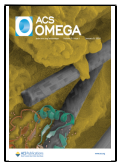

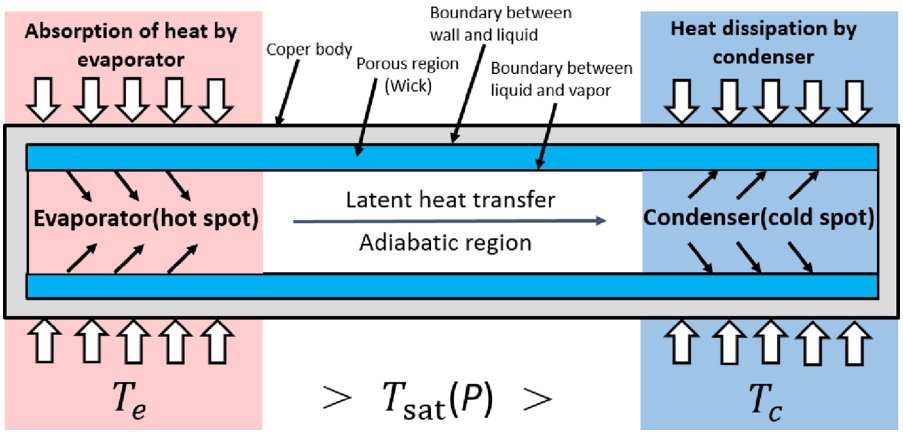

Figure 1. Schematic diagram of heat pipe. Reprinted with permission from ref 23. Copyright 2021 Elsevier.

operation of Li-ion batteries is 15 to 40 °C.[9] With temperatures higher than 50 °C, the operation efficiency of Li-ion batteries would become obviously lower and the life span would be shortened accordingly.[10] When temperature rises to 70 °C or higher, thermal runaway and safety issues may occur.[11] Therefore, a thermal management system is essential to avoid heat accumulation in Li-ion batteries, especially for high-power Li-ion batteries applied to electrified vehicles.

The most commonly used cooling techniques in battery thermal management systems (BTMSs) include air cooling, liquid cooling, phase change material (PCM) cooling, heat pipe cooling, and combinations of one or more of these techniques. Among all kinds of BTMSs, air-cooled BTMSs are superior to other kinds of BTMSs in view of their simple structure, low cost, and easier maintenance.[12] However, for large battery packs, the heat transfer coefficients and cooling uniformity of air-cooled BTMSs could not meet the requirements of heat removal; in this case, liquid-cooled BTMSs with more efficient heat removal performance should be applied.[13] The structures of liquid-cooled BTMSs are more complex than air-cooled ones as some components, such as cooling plates with liquid channels and pumps, are added. This may in turn increase the mass, volume, and cost of BTMSs.[14−16] Besides, leakage problems may exist in liquid-cooled BTMSs, which could further lead to a short circuit and thermal runaway. BTMSs based on PCM have been more attractive these years due to their advantages in energy-saving and low maintenance cost. PCM could absorb a large amount of latent heat when changing from solid phase to liquid phase. Thus, batteries could maintain around the phase change temperature for a long time and prevent the quick temperature rise phenomena.[17,18] However, for Li-ion batteries used for long-run operation, long discharging processes are inevitable, PCM will turn into liquid phase completely, and the heat absorption ability will become much weaker. Under this circumstance, heat dissipation of Li-ion batteries is highly dependent on the thermal conductivity of PCM. If paraffin is used as the PCM in BTMSs, issues of low structural strength, low thermal conductivity, and high leakage risk are associated, restraining the commercial use of PCM cooled BTMSs.[19] Though adding foam-metal or using expanded graphite(EG)/paraffin composite instead of pure paraffin could raise the structural strength, improve the thermal conductivity, and reduce the risk of leakage of PCM cooling BTMSs, the heat stored in PCM could not be easily evacuated. Consequently, if air-cooling and liquid cooling techniques are used in combination of PCM cooled BTMSs, this kind of BTMSs could be more applicable.[20−22]

In recent years, BTMSs based on heat pipes have been extensively investigated owing to their advantages in thermal conductivity, compactness, and maintenance effort. Generally, heat pipes have three main sections, i.e., evaporator, adiabatic region, and condenser (Figure 1). In the evaporator section, heat will transfer from Li-ion batteries to heat pipes, and liquid in the wick structure will experience the transition from liquid phase to gas phase. The evaporated liquid then passes through the adiabatic region and reaches the condensation section. In the condensation section, the heat of vapor will dissipate from the heat pipe to the outside and vapor will turn into liquid again. Afterward, the condensate will return to the evaporator section influenced by the capillary force of wick. It is apparent that the efficiency of the condensation section is critical for the cooling performance of the heat pipe based BTMSs. Hence, other cooling methods should be used to aid in the heat evacuation of the condensation section. In this case, optimized performance of heat pipe cooled BTMSs could be achieved.

Generally, heat pipes applied to BTMSs could be classified as flat single-channel heat pipes, oscillating heat pipes, flexible heat pipes, and microchannel heat pipes. Flat single-channel heat pipes have the advantages of easier manufacture and lower cost. Oscillating heat pipes could achieve efficient cooling with smaller volume and, thus, are more adaptable to BTMSs with condensed space. Flexible heat pipes being lightweight could achieve different configurations and, thus, to some extent, could lead to space-saving BTMSs. Microchannel heat pipes, normally manufactured in a flat shape, have higher heat transfer capability and improved cooling uniformity than flat single-channel heat pipes with raised manufacture complexity. All of these types of heat pipes have their advantages and, therefore, have been widely used in BTMSs for Li-ion batteries.

Though BTMSs based on heat pipes have drawn great attention in recent years, systematic review work focused on this type of BTMSs has not yet been conducted yet. In this paper, investigations concerning the application of BTMSs based on four different types of heat pipes, i.e., flat single-channel heat pipes, oscillating heat pipes, flexible heat pipes, and microchannel heat pipe, have been analyzed from the effects of cooling method, geometry parameter, working fluid, filling ratio, etc. The techniques for the visualization of the flow behavior inside oscillating heat pipes and the methods for the realization of heat pipe flexibility have also been summarized. The contents of this paper could give guidance for the choice

https://doi.org/10.1021/acsomega.3c08056
ACS Omega 2024, 9, 97−116

Table 1. Investigations of BTMSs Based on Flat Single-Channel Heat Pipes

Battery Type	Nominal Capacity per Cell	Nominal Voltage per Cell	Cooling Method	Working Fluid	Focus of Investigation	Research Method	Source
Rectangular $LiFePO_4$ battery	8 A·h	-	Water cooling	Water	Effects of input power and inclination angle.	Experiment	Rao et al. 2013[24]
Li-ion Battery pack with 14 cylindrical cells	7 A·h	-	Natural/forced air cooling	Water	Comparison between cooling systems based on heat sink and heat pipe combined with heat sink; effects of air velocity and inclination angle.	Experiment and 1D simulation	Tran et al. 2014[25]
Prismatic Li-ion battery	10 A·h	-	Forced air cooling/water cooling	Water	Effects of cooling water flow rate, number of heat pipes, copper fins and heat spreaders; feasibility of air-cooling method.	Experiment and 3D simulation	Ye et al. 2015[26]
Li-ion battery simulators(2 containers with 4 cartridge heaters)	2.5−40W per simulator	-	Glycol-water cooling	Water	Effects of discharge rate and transient cycles.	Experiment	Wang et al. 2015[27]
Li-ion battery pack with 5 prismatic cells	12 A·h	3.2 V	Forced air cooling/PCM cooling+ forced air cooling	Water	Effects of discharge rate and mass flow rate of cooling air velocity; comparison between the cooling performance of BTMS based on PCM, heat pipe assisted PCM and heat pipe assisted PCM with forced air cooling.	Experiment	Wu et al. 2017[28]
$Li(NixCoyMnz)O_2$ battery pack with 4 pouch cells	24 A·h	-	Water cooling	Water	Effects of heating power and mass flow rate of cooling water; capability of the prevention of thermal runaway propagation.	Experiment	Wang et al. 2019[29]
Li-ion battery pack with 3 prismatic cells	10 A·h	3.2 V	Natural air cooling	Water	Effects of discharge rate and state of charge(SOC) on the occurrence of thermal runaway; the detailed process of thermal runaway propagation.	3D simulation	Li et al. 2019[30]
Li-ion battery pack with 36 prismatic cells	42 A·h	-	Water cooling with additional cooler	Water	Effects of discharge rate and additional cooler.	3D simulation	Xu et al. 2019[31]
$LiFePO_4$ battery pack with 5 prismatic cells	8.5 A·h	3.2 V	Natural air cooling	Acetone	Effects of discharge rate and cooling method.	Experiment and 3D simulation	Zhang and Wei 2020[32]
Li-ion battery module with 2 prismatic cells	4.4 A·h	3.7 V	Water cooling	Water	Effects of battery surface temperature and cooling water velocity.	Experiment and 3D simulation	Alihosseini and Shafaee 2021[23]
$Li(Ni_{1/3}Co_{1/3}Mn_{1/3})O_2$ battery pack with 2 cells	25 A·h	3.6 V	PCM cooling+water cooling	Water	Sensitivity analysis of geometry parameters and cooling water velocity; optimization design of the key parameters; thermal runaway behavior of different designs.	Experiment and 3D simulation	Zhang et al. 2021[33]
Li-ion battery pack with 5 pouch cells	53 A·h	-	Forced air cooling/water cooling	Water	Effects of cooling method, manufacturing tolerance and battery aging.	3D simulation	Liang et al. 2021[34]
Li-ion battery simulators(36 cylindrical heaters)	-	-	PCM cooling+water cooling	Acetone	Effect of heating power and cooling water temperature.	Experiment and 2D simulation	Abbas et al. 2021[35]
$Li(Ni_{1/3}Co_{1/3}Mn_{1/3})O_2$ Battery pack with 18 cylindrical cells	4 A·h	-	PCM cooling+natural air cooling	-	Effects of cooling method and battery center distance.	3D simulation	Tang et al. 2022[36]
Li-ion battery simulator	4.9−73.2 W per simulator	-	Natural air cooling/water cooling	3 M Novec 649	Effects of discharge rate, cooling method and uniform heat ratio.	Experiment	Jang et al. 2024[37]

https://doi.org/10.1021/acsomega.3c08056
ACS Omega 2024, 9, 97−116

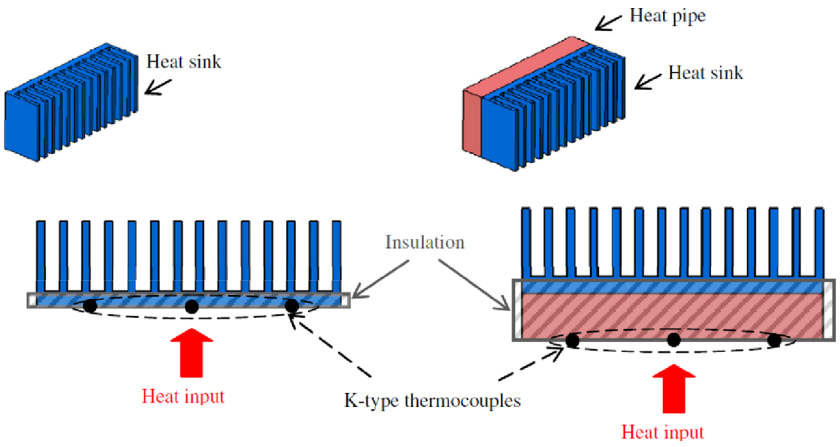

Figure 2. Schematic diagram of cooling systems based on heat sink and heat sink combined with heat pipe. Reprinted with permission from ref 25. Copyright 2014 Elsevier.

and design of BTMSs based on heat pipes for Li-ion batteries. Besides, the research limitations of the current research works have also been pointed out, and directions for the future work have been given.

2. BTMSS BASED ON FLAT SINGLE-CHANNEL HEAT PIPES

Since the geometry of flat single-channel heat pipes is simple, most studies focused on BTMSs based on flat single-channel heat pipes are concentrated on the evaluation and choice of the cooling method. There are two primary research focuses when different cooling methods are applied, one is cooling performance, and the other is thermal runaway characteristics. Investigations of BTMSs based on flat single-channel heat pipes are summarized in Table 1.

2.1. Effects of Cooling Method on Cooling Performance. Cooling performance is the most concerning point of BTMSs based on flat single-channel heat pipes with different cooling methods. Tran et al.[25] compared the cooling performance of BTMS with only heat sink and BTMS with both heat sink and heat pipe(Figure 2); as indicated by their results, the thermal resistance of cooling system could be reduced by 30% when a flat single-channel heat pipe is added at conditions with natural air convection; when forced air convection is applied, the positive effects of the heat pipe will be reduced; they also pointed out that the inclination angle affects the cooling performance slightly when heat pipes are not over charged, implying that the position and road grade have limited effects on cooling performance of BTMSs based on flat single-channel heat pipes with lower filling ratios. Rao et al.[24] analyzed the temperatures at different locations and the maximum temperature differences of a $LiFePO_4$ battery based on heat pipes with flat shaped evaporator and water cooling method; as indicated by their results, the temperatures of the battery could be controlled within 50 °C and temperature differences could be maintained within 5 °C if input power is lower or equal to 30 W; besides, smaller temperature differences compared to those with horizontally placed heat pipes could be achieved when the heat pipe is placed vertically. Ye et al.[26] along with Alihosseini and Shafaee[23] found that increasing mass flow rate of cooling water as well as adding copper fins could improve the cooling performance in terms of reducing temperature rise and improving temperature uniformity; raising the number of heat pipes could lead to increases in the heat transfer area; however, deteriorated thermal uniformity is associated with this. Adding the vortex generator has beneficial effects on thermal uniformity, whereas the heat transfer coefficient would be lower. As also suggested by their results, forced air cooling may be feasible for battery units but could not meet the cooling requirements of battery packs with high discharge rates. In the study of Zhang and Wei[32] as well as Jang et al.,[37] the superiority of BTMS based on a flat single-channel heat pipe with respect to the control of temperature rise and temperature uniformity was further confirmed; the authors pointed out that the temperature increase of the batteries is lower than 15 °C at discharge rates in the range of 1C to 6C (C-rate is the measurement of the charge and discharge current with respect to its nominal capacity) and the temperature difference within the battery pack is below 5 °C at discharge rates of 2C and 4C or during cyclic operation when flat single-channel heat pipes combined with natural air convection or water cooling are adopted. These, however, could not be realized by aluminum plate cooling combined with natural air convection. Nevertheless, as indicated by the research work of Wang et al.,[27] when a transient cycle with periods of high discharge rates (higher than or equal to 4C) are considered, temperature rise could not be controlled below 27 °C when a BTMS based on flat single-flat heat pipe combined with liquid cooling is adopted; this implies that better designs or improved cooling methods should be considered for BTMSs based on flat single-channel heat pipes.

For a larger battery pack investigated by Xu et al.,[31] using a flat single-channel heat pipe combined with water cooling is not sufficient for the requirement of heat dissipation, additional coolers are essential. Meanwhile, as found by Liang et al.,[34] the cooling demand will increase markedly when a battery pack with large manufacture tolerance and aged cells is applied. To achieve better control of temperature for large battery packs operating at transient cycles, Wu et al.,[28] Zhang et al.,[33] Abbs et al.,[35] and Tang et al.[36] adopted BTMSs based on flat single-channel heat pipes combined with a phase change material (PCM) plate and air cooling or water cooling method (Figure 3); their results showed that when this new type of BTMSs is applied, battery temperature could be much lower than that of the BTMS based on only PCM, implying that the application of a hybrid cooling method is beneficial for the heat evacuation for Li-ion batteries. It should also be noticed that most studies

https://doi.org/10.1021/acsomega.3c08056
ACS Omega 2024, 9, 97−116

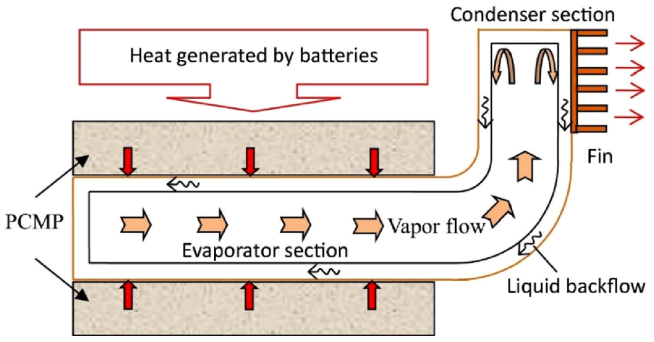

Figure 3. Schematic diagram of BTMS based on heat pipe combined with PCM plate and forced air cooling method. Reprinted with permission from ref 28. Copyright 2017 Elsevier.

regarding BTMS based on flat single-channel heat pipes are designed for prismatic or pouch batteries. For cylindrical batteries used in the study of Abbs et al.[35] and Tang et al.,[36] the gap between the flat single-channel heat pipes and cylindrical batteries and the gap between cylindrical batteries are important influencing factors; as indicated by their results, the spacing between cells and the spacing between cells and heat pipes should be appropriately designed to ensure cooling performance and temperature uniformity and system compactness. In summary, for BTMSs based on flat single-channel heat pipes, using liquid cooling could achieve improved heat transfer characteristics compared to natural/forced air cooling; for large battery packs with high power-output, the addition of PCM and additional cooler may be essential.

2.2. Effects of Cooling Method on Thermal Runaway. With the benefits in heat conductivity, BTMS based on the flat heat pipe and water cooling method was also proven to be capable of preventing the propagation of thermal runaway by Wang et al.[29] and Li et al.[30] As indicated by their results, once thermal runaway occurs in one cell, the heat generated could dissipate rapidly and will not trigger the thermal runaway of other cells. Besides, as pointed out by Zhang et al.,[33] the cooling performance of BTMS based on the PCM and water cooling method could be improved when the heat pipe is adopted, and heat dissipation could be further promoted when the key parameters are systematically optimized. In this case, it could be concluded that the risk of thermal runaway could be reduced with the application of BTMS based on the combined used of PCM, heat pipe, and water cooling.

3. BTMSS BASED ON OSCILLATING HEAT PIPES

Oscillating heat pipes are featured by structures consisting of winding capillary tubes or channels, which are partially filled with liquid working fluids. Different from BTMSs based on flat heat pipes, BTMSs based on oscillating heat pipes could avoid the use of wick structures and could reduce the cost of manufacture. Additionally, more efficient heat dissipation could be achieved by using an oscillating heat pipe instead of a conventional heat pipe.

BTMSs based on oscillating heat pipes could be classified as open loop systems and closed loop systems. Closed loop systems are more attractive due to their better cooling performance. A typical schematic of BTMS based on oscillating heat pipe is shown in Figure 4 and investigations on the cooling performance of BTMSs based on oscillating heat pipes are summarized in Table 2.

3.1. Effects of Geometry Parameters. For oscillating heat pipes, the geometry of the tubes has significant effects on the cooling characteristics. Important geometry parameters of oscillating heat pipes include number of turns, the length of different sections, inner hydraulic diameter etc. Normally, increasing the number of turns could result in enhanced oscillation and circulation of the liquid slugs and vapor plugs; subsequently, the thermal resistance at high heating power would be reduced.[63,64] Expect for increasing number of turns, heat transfer of oscillating heat pipes could be improved by using a smaller ratio between the length of evaporator section and hydraulic diameter.[40] It was also pointed out that quick

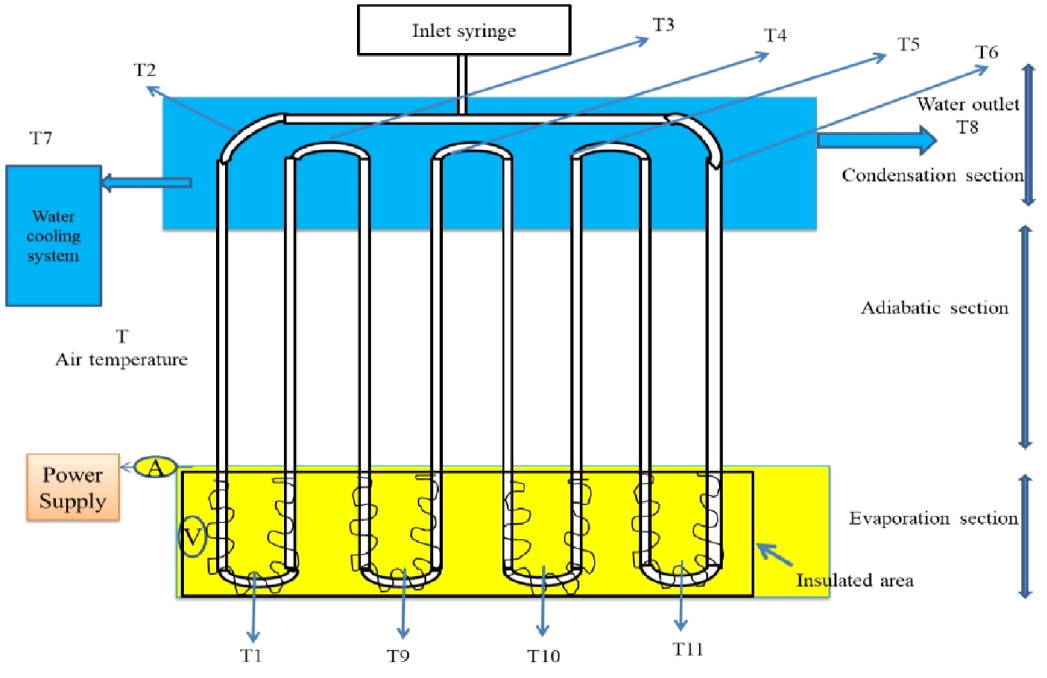

Figure 4. A typical schematic of BTMS based on oscillating heat pipe. Reprinted with permission from ref 38. Copyright 2021 Elsevier.

https://doi.org/10.1021/acsomega.3c08056
ACS Omega 2024, 9, 97−116

Table 2. Investigations on the Cooling Performance of BTMSs Based on Oscillating Heat Pipes

Heat source	Heating power	Cooling method	Working fluid	Focus of investigation	Research method	Source
Heating wire	10−60 W	Natural air cooling	FC-72/ethanol/water	Effects of heating power, working fluid and filling ratio.	Experiment	Zhang et al. 2004[39]
Hot water bath with temperature of 80 °C	/	Constant temperature water bath	R123/ethanol/water	Effects of hydraulic diameter and the ratio of length of evaporation section to hydraulic diameter.	Experiment	Rittidech et al. 2007[40]
Hot water bath	/	Constant temperature water bath	Water/methanol/ethanol/acetone	Effects of inner surface cavity size and working fluid.	Experiment and simulation based on theoretical model	Qu and Ma 2007[41]
Heating wire	8−145 W	Constant temperature water bath	Water	Effects of hydraulic diameter and length of adiabatic section.	Experiment	Lin et al. 2011[42]
Heating wire	10−100 W	Forced air cooling	Water/acetone/water-acetone mixtures	Effects of heating power and working fluid.	Experiment	Zhu et al. 2014[43]
Rectangular electric heater	20−40 W	Constant temperature water bath	Acetone	Effects of heating power and inclination angle.	Experiment	Rao et al. 2014[44]
Heating wire	10−120 W	Constant temperature water bath	Water/heptanol solution	Effects of heating power, inclination angle and working fluid.	Experiment	Hu et al. 2014[45]
Rectangular electric heater	10−160 W	Constant temperature water bath	Kerosene/Fe_2O_3 nanofluid.	Effects of nanofluid charging and magnetic field.	Experiment	Goshayeshi et al. 2015[46]
Rectangular electric heater	10−100 W	Constant temperature water bath	Deionized water/n-butanol aqueous solution/graphene oxide nanofluid/mixed graphene oxide and n-butanol alcohol aqueous solutions	Effects of working fluids and heating power.	Experiment	Su et al. 2016[47]
Rectangular electric heater	20−45 W	Constant temperature water bath	Acetone	Effects of PCM and inclination angle.	Experiment	Wang et al. 2016[48]
Rectangular electric heater	5−65 W	Constant temperature water bath	Deionized water	Effects of heating power, inclination angle and location of the condensation section.	Experiment	Rao et al. 2017[49]
Heating wire	15−60 W	Constant temperature water bath	Water/ethanol/heptanol solution	Effects of working fluid and inclination angle.	Experiment	Zhao et al. 2018[50]
Two rectangular electric heaters	30−100 W	Aluminum block with water flowing channels	Methyl perfluoroisobutyl ether (HFE-7100)	Effects of heating power, filling ratio and temperature difference between two heat sources.	Experiment	Jang et al. 2018[51]
Rectangular electric heater	10−25 W	Cooling plate cooled by constant temperature cooling water	Ethanol	Effects of heating power, filling ratio and inclination angle.	Experiment	Chi et al. 2018[52]
Rectangular electric heater	80−120 W	Cooling plate cooled by constant temperature cooling water	Deionized water	Effects of heating power and structure of oscillating heat pipe.	Experiment	Qu et al. 2019[53]
Rectangular electric heater	60−300 W	Cooling plate cooled by constant temperature cooling water	Water/ethanol/acetone	Effects of heating power and working fluid.	Experiment	Hao et al. 2019[54]
Two rectangular electric heaters	8−56 W	Forced air cooling	Ethanol/ethanol−water mixtures/water	Effects of filling ratio and working fluid.	Experiment	Wei et al. 2019[55]
Rectangular electric heater	10−20 W	Cooling plate cooled by constant temperature cooling water	Methanol	Effects of heating power, inclination angle, inner hydraulic diameter and filling ratio.	Experiment	Chi and Rhi 2019[56]
Heating wire	20−60 W	Constant temperature water bath	Ethanol−water mixtures/graphene nanofluids/surfactant aqueous solutions/deionized water	Effects of heating power and working fluid.	Experiment	Xu et al. 2020[57]
Lithium-ion battery module with capacity of 68A·h	Discharge rate from 0.5C to 1.5C	Natural air cooling	Deionized water/water-based TiO_2 nanofluid	Effects of ambient temperature and battery discharge rate.	Experiment	Chen and Li 2020[58]
Rectangular electric heater	25−100 W	Forced air cooling	Deionized water	Effects of heating power, 3D structure and cooling air velocity.	Experiment	Ling et al. 2020[59]

https://doi.org/10.1021/acsomega.3c08056
ACS Omega 2024, 9, 97−116

Table 2. continued

Heat source	Heating power	Cooling method	Working fluid	Focus of investigation	Research method	Source
Electric heating plate	5–40 W	Constant temperature water bath	Ethanol-pentane mixtures	Effects of heating power, inclination angle and working fluid.	Experiment	Markal and Varol 2020[60]
Four heating blocks	40–640 W	Forced air cooling	Acetone	Effects of heating power and inclination angles.	Experiment	Liu et al. 2020[61]
Rectangular electric heater	8–56 W	Forced air cooling	Ethanol–water mixture/ethanol aqueous solutions of carbon nanotubes	Effects of heating power and working fluid.	Experiment	Zhou et al. 2021[62]
Heating wire	20–140 W	Constant temperature water bath	Deionized water/hexanol solution	Effects of heating power and filling ratio.	Experiment	Singh and Kumar 2021[38]

start up and reduced thermal resistance could be achieved by using a length ratio between the evaporator and condenser higher than 1.0.[65] Adopting a larger hydraulic diameter, shorter length of adiabatic section, and rougher inner surface of the capillary tube could also improve the start-up performance, whereas an excessive large hydraulic diameter would lead to increased working fluid and increased thermal resistance when an oscillating heat pipe is horizontally placed.[40−42] Additionally, using a larger hydraulic diameter and square channel instead of circular channel could extend the upper operating limit, which means the oscillating heat pipes with larger hydraulic diameter and square channel could be adaptable to batteries with higher power output.[66] Furthermore, when heat pipes are horizontally placed, the thermal resistance of the oscillating heat pipe is larger than multiple single-channel heat pipes, whereas, an opposite trend could be observed when the heat pipes are vertically placed at high heating powers,[42] which means that the advantages of oscillating heat pipes are more obvious when BTMSs are horizontally placed.

3.2. Effects of Battery Placement Method and Inclination Angle. To disclose the effects of the placement method of BTMS based on an oscillating heat pipe, Rao et al.,[44,49] Hu et al.,[45] Wang et al.,[48] and Chi et al.[52,56] designed BTMS based on oscillating heat pipes cooled by water bath or cooling plate. They found that the cooling performance could be improved when the battery terminal is placed upward with appropriate distance between the evaporator section and condensation section. Meanwhile, the reflow of working fluid could be aided if the oscillating pipe is vertically placed, and heat resistance would be increased if the oscillating pipe is inclined to the horizontal direction. However, during the real operation process of BTMS based on oscillating heat pipes equipped on electric vehicles, the inclination of the oscillating heat pipes is inevitable; thus, it is recommended that the road slope should be taken into consideration when evaluating the cooling performance of oscillating heat pipes.

3.3. Effects of Working Fluid. For oscillating heat pipes, the working fluid has great influences on the heat transfer characteristics. The frequently used working fluids of oscillating heat pipes include water, acetone, alkanes with high carbon numbers, alcohols, nanofluids, surfactant aqueous solutions, and fluorinated liquid. Properties for the most frequently used working fluids in oscillating heat pipes are listed in Table 3. Generally, the working fluid chosen for oscillating heat pipes should have lower latent heat to ensure the fast bubble generation and growth processes, high specific heat to raise the total heat brought by the working fluid, and lower dynamic viscosity and surface tension to reduce flow resistance. Zhang et al.[39] compared the cooling performance of copper oscillating heat pipe charged with FC-72, ethanol, and water at a heating power lower than 60 W; their results suggested that FC-72 is more adaptable to batteries with power lower than 20 W while for batteries with power higher than 20 W, water is a more preferable choice. Qu and Ma[41] compared the start-up characteristics of a glass oscillating heat pipe charged with water, methanol, ethanol, and acetone; they found that the heat flux needed for the start-up of the oscillating heat pipe charged with water is much larger than those for the start-up of oscillating heat pipe charged with methanol, ethanol, and acetone; when methanol is selected as the working fluid, the heat flux needed for start-up would be the lowest among all these working fluids. Hao et al.[54] compared the cooling performance of polytetrafluoroethylene

https://doi.org/10.1021/acsomega.3c08056
ACS Omega 2024, 9, 97−116

Table 3. Properties of the Working Fluids Used in Oscillating Heat Pipes[39,54,60]

Fluids	Boiling point (°C)	Liquid density (kg/m^3)	Surface tension (×10^3) (N/m)	Vapor pressure at 100 °C(Pa)	Latent heat of vaporization (kJ/kg)	Liquid dynamic viscosity (× 10^3) (Pa·s)	Specific heat (J/kg·°C)	Liquid thermal conductivity (W/m·°C)
Water	100	958	58.91	1.01 × 10^5	2256.7	1.01	4217	
Ethanol	78.3	757	17.46	2.26 × 10^5	960.0	1.15	2580	0.172
FC-72	56.6	1600	8.35		94.8		1102	
Pentane	36.06	625.5	15.8		366.9	0.242	2330	0.138
Acetone	56.2	792	23.7	4.43 × 10^5	523	0.320	2350	0.170

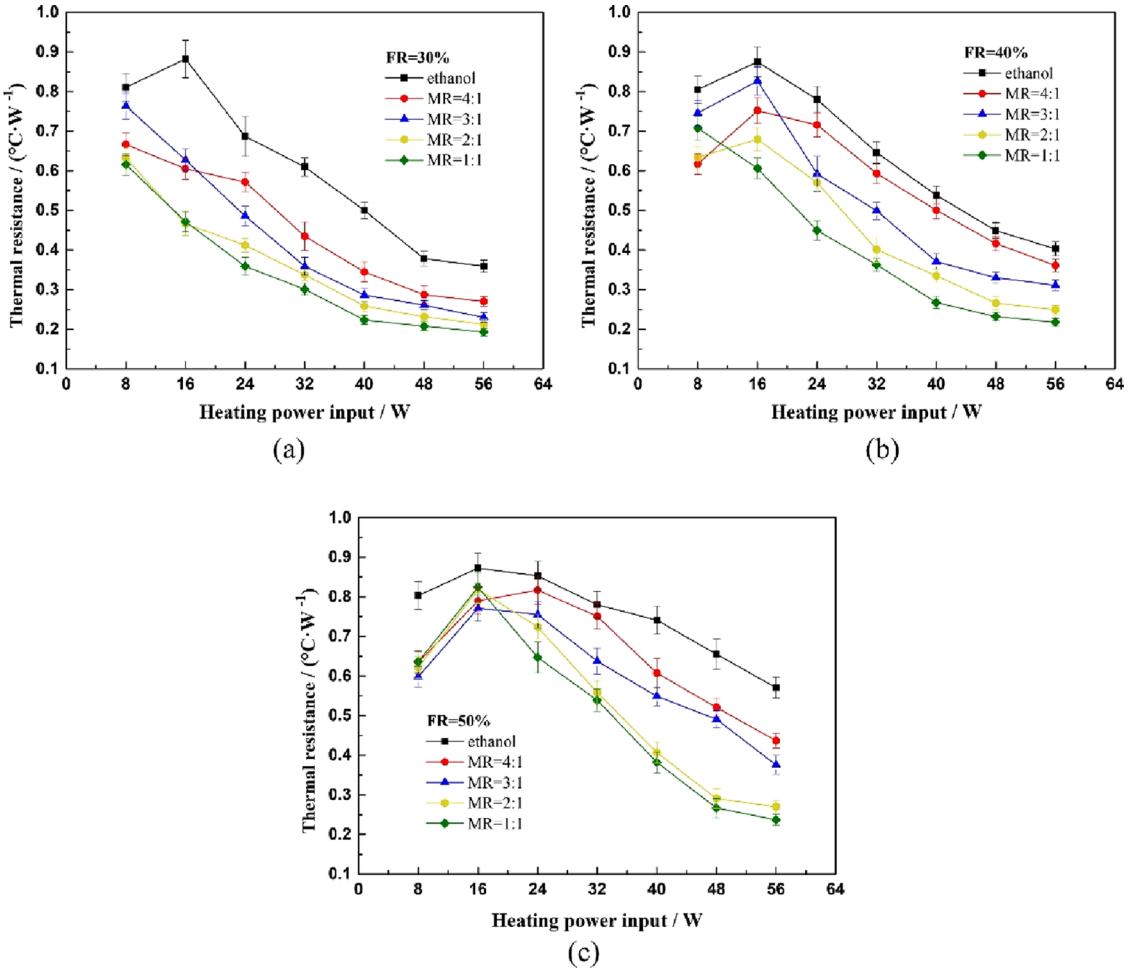

Figure 5. Variations of thermal resistance for oscillating heat pipe charged with ethanol−water mixtures at different mixing ratios: (a) FR = 30%; (b) FR = 40%; (c) FR = 50%. Reprinted with permission from ref 55. Copyright 2019 Elsevier.

oscillating heat pipe charged with water, ethanol, and acetone at a heating power in the range of 60−300 W; as indicated by their results, acetone reveals the highest heat transfer coefficient and the lowest heat resistance in the whole heating power range tested, while water seems to be the worst choice. The diversities in the conclusions of these studies may be due to the differences in the material and size of oscillating heat pipes; the better cooling performance observed when water is used as the working fluid in the copper oscillating heat pipe could be attributed to the reduced capillary resistance of water when contacted with the hydrophilic copper surface. It could be also allowed that the choice of working fluid is highly dependent on the surface treatment method of the capillary tube inner surface, as the hydrophilicity and the subsequent capillary resistance could be easily changed by the surface treatment method.

Since each liquid has its pros and cons, binary mixtures of the above-mentioned working fluids may have better thermosphysic properties and thus could gain better cooling performance. To disclose the potential of the binary mixtures, Zhu et al.[43] investigated the operation characteristics of an oscillating heat pipe filled with different mixing ratios of water and acetone. As manifested by their results, the addition of acetone into water could lead to improved start-up performance. At lower filling ratios, mixing acetone into water could result in reduced thermal resistance at higher heating powers; however, at higher filling ratios, mixing acetone into water would result in increased thermal resistance at higher heating powers. Wei et al.[55] tested the heat transfer performance of an oscillating heat pipe filled with different mixing ratios of ethanol and water. They found that ethanol−water mixtures have better transport characteristics than pure water or ethanol and thus

https://doi.org/10.1021/acsomega.3c08056
ACS Omega 2024, 9, 97−116

could be regarded as a promising choice of working fluid for oscillating heat pipes (Figure 5). Among all the ethanol−water mixtures, the mixture with 1:1 mixing ratio seems to have the lowest thermal resistance at the most heating power. Markal and Varol[60] investigated the working behavior and cooling performance of an oscillating heat pipe charged with an ethanol−pentane mixtures; they found that using a mixture with a high pentane fraction (i.e., 75%) as working fluid could attain better cooling performance than other mixtures with a lower pentane mixing ratio (25% and 50%).

When nanoparticles are added into the liquid, the thermal conductivity of the working fluid is improved owing to the effects of Brownian motion and the large specific surface area. Goshayeshi et al.[46] investigated the cooling performance of a BTMS based on oscillating heat pipes filled with a kerosene/Fe_2O_3 nanofluid. As indicated by their results, use of a heat pipe charged with the kerosene/Fe_2O_3 nanofluid could achieve up to 14% reduction in heat resistance compared with that of a heat pipe charged with pure kerosene when a magnetic field is not present, while up to 27% reduction in heat resistance could be achieved when a heat pipe charged with kerosene/Fe_2O_3 nanofluid is exposed to a magnetic field, implying that the combined use of kerosene/Fe_2O_3 nanofluid and external magnetic field could improve the cooling performance by a large extent. TiO_2 particles have similar beneficial effects on heat transfer as Fe_2O_3 particles. As pointed out by Chen and Li,[58] after adding TiO_2 particles into deionized water, the thermal resistance could be reduced by more than 30% and the temperature uniformity could also be substantially improved. Apart from metal oxide nanoparticles, nanoparticles made by carbon materials are also considered to be capable of enhancing the heat transfer performance of working fluids used in oscillating heat pipes. Hu et al.,[45] Su et al.,[47] and Zhao et al.[50] as well as Singh and Kumar[38] compared the cooling performance of BTMS based on oscillating heat pipes filled with water, ethanol, rewetting fluids, water-based graphene oxide nanofluids, and self-rewetting nanofluids. As indicated by their results, adoption of self-rewetting fluids instead of water or ethanol as well as adding graphene oxide nanoparticles into water or self-rewetting fluids could improve heat transfer characteristics. The beneficial effects of self-rewetting fluids (aqueous solutions of alcohols with carbon number higher than 4) on heat transfer are mainly attributed to the nonlinear behavior of surface tension with the increase of temperature, which could enhance the movement of liquid from the condenser section to the evaporator section at high temperatures.[67] However, the improvement of heat transfer when graphene oxide nanoparticles are added could be attributed to the increase in thermal conductivity. Since using mixtures of ethanol and water as well as nanoparticles could both lead to enhanced heat transfer, it could be allowed that adding nanoparticles to ethanol−water mixtures could reduce thermal resistance and improve cooling performance. Xu et al.[57] and Zhou et al.[62] mixed graphene nanoparticles or multiwall carbon nanotubes with an ethanol−water mixture and found that the cooling performance could be significantly improved if the proportion of nanoadditives is appropriately selected. However, most of the studies mentioned here concerning the use of nanofluids in oscillating heat pipes were focused on the heat transfer enhancement behavior; the possibly induced negative effects, such as the stability of the nanofluids, the deposition of nanoparticles on inner walls, and the wear of the inner wall material, were not systematically studied.

3.4. Effects of Filling Ratio. Filling ratio is also regarded as a key influencing factor for oscillating heat pipes as indicated by the results of Su et al.,[47] Jang et al.,[51] Singh and Kumar,[38] and Chi and Rhi.[56] The optimum filling ratio is dependent on the type of working fluid, heating power, inner hydraulic diameter, and temperature difference in the evaporator section. It is indicated by the results of Chi et al.[52,56] that when ethanol or methanol is adopted as the working fluid in oscillating heat pipes and heating power is lower than 25 W, optimized cooling performance could be obtained when the filling ratio is in the range of 2%−26%, and the optimum filling ratio decreases with the increase of inner hydraulic diameter. As concluded by Zhang et al.,[39] Sun et al.,[68] and Kang et al.,[69] if FC-72, ethanol, and water are adopted as the working fluid for oscillating heat pipes at a heating power up to 110 W, using a filling ratio of 70% could obtain the best cooling performance. When HFE-7100 is chosen as the working fluid, an oscillating heat pipe with a lower filling ratio of 50% seems to perform better with lower heating powers and smaller temperature differences in the evaporator section. At higher heating powers and larger temperature differences in the evaporator section, using higher filling ratios of 60% or 70% tends to be a more preferable choice in terms of heat transfer and elimination of early dry-out.[51] For binary mixtures, such as ethanol−water mixtures and ethanol−pentane mixtures used in the studies of Wei et al.[55] as well as in those of Markal and Varol,[60] the optimum filling ratio is 30% (Figure 5). As could be induced from the above studies, the optimum filling ratio obtained for one working fluid could not be used for another, which means that the effects of the filling ratio should be evaluated for different working fluids. However, detailed studies regarding the effects of filling ratio have not been conducted for nanofluids and self-rewetting fluids yet.

3.5. Effects of Adding PCM and Structure Optimization. Except for the optimization of the placement method, working fluid, and filling ratio, measures such as adding PCM and structure optimization could also be taken to further improve the cooling performance of BTMS based on oscillating heat pipes. Wang et al.[48] used PCM combined with oscillating heat pipe in the BTMS system. As indicated by their results, temperature rise could be restrained by the combined use of oscillating heat pipe and PCM, whereas the temperature difference may be enlarged. Thompson et al.[70] proved that adding Tesla check valves to an oscillating heat pipe could promote the circulation of liquid slugs in the evaporation section and subsequently reduce the thermal resistance. Qu et al.[53] designed oscillating heat pipes with PCM and 3-layer or 4-layer 3D structures; their results showed that better cooling performance could be achieved if 3D oscillating heat pipes are adopted instead of multiple 2D oscillating heat pipes (Figure 6). Ling et al.[59] compared the heat transfer characteristics of oscillating heat pipes with a 4-layer 3D structure and leaf-shaped structure (Figure 7); as indicated by their results, lower thermal resistance and 2% improvement in cooling efficiency could be achieved when a leaf-shaped structure is adopted. Liu et al.[61] designed an oscillating heat pipe with dual-serpentine-channel (Figure 8); they compared the thermal resistances of an oscillating heat pipe with dual-serpentine-channel to those of an aluminum alloy plate with the same geometry and found that at most heating powers, the thermal conductivity of the oscillating heat pipe with dual-serpentine-channel are 5.8 times (averaged value) larger than those of aluminum alloy plate with less

https://doi.org/10.1021/acsomega.3c08056
ACS Omega 2024, 9, 97−116

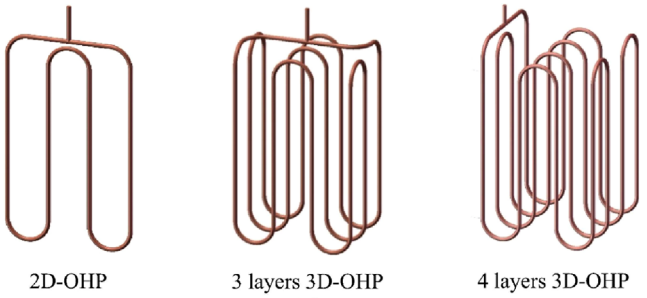

Figure 6. Schematic of two-dimensional (2D) oscillating heat pipe (OHP), 3 layers three-dimensional (3D) OHP, and 4 layers 3D OHP. Reprinted with permission from ref 53. Copyright 2019 Elsevier.

weight; however, they did not compare the cooling performance of the oscillating heat pipe with a dual-serpentine-channel to that of an oscillating heat pipe with a single-serpentine-channel, which is a more frequently used structure of oscillating heat pipes.

Different from the above studies, which used electric heaters or heating wires as the heat source, Chen and Li[58] adopted an oscillating heat pipe with a Li-ion battery as the heat source; under this circumstance, the working condition is more realistic as temperatures near the anode and cathode are higher for a real battery. It is manifested by their results that the temperature rise and temperature uniformity of a battery equipped with BTMS based on an oscillating heat pipe could be controlled within acceptable range if the discharge rate is not higher than 1.5C. Liu et al.[71] managed to use oscillating heat pipes on a Li-ion battery pack. They adopted two different schemes, i.e., multiple small-scale oscillating heat pipes and one large-scale oscillating heat pipe. Their results indicated that multiple small-scale oscillating heat pipes showed better performance in terms of temperature rise inhibition, while one large-scale oscillating heat pipe could achieve better temperature uniformity. Kang et al.[69] tried to enhance the heat transfer of the oscillating heat pipe by adding separating walls in the flow channel. Their results indicated that the optimal location of separating walls varies with filling ratio; at high filling ratio of 70%, the highest thermal conductivity of the oscillating heat pipe could be obtained when the separating walls were located at the middle of the flow channel, whereas at lower filling ratios, better heat transfer performance could be obtained when the separating walls were located near the inner side of the flow channel.

3.6. Visualization of Inside Flow Movement. The above-mentioned works were focused on the investigations of temperature distribution, temperature rise, heat flux, and heat transfer resistance in oscillating heat pipes. The detailed fluid movement was not included. To disclose the flow characteristics of the oscillating heat pipes, Tong et al.,[72] Kim et al.,[63] Xu et al.,[73] and Senjaya and Inoue[74] along with Sun et al.[68] used oscillating heat pipes made by Pyrex glass to realize the visualization of the inside flow patterns (Figure 9); as indicated by their results, fierce oscillations in the heat pipes occur during the start-up period, after which, the flow pattern would change to continuous circulation with local oscillations. The size and movement of bubbles in the oscillating heat pipes are closely associated with the type of working fluid, while the heat transfer could be highly enhanced only during the generation and growth of tube-sized bubbles or vapor plugs rather than the generation of small bubbles. Kim et al.[64,66,75,76] investigated the inside flow movement of oscillating heat pipes by engraving the flow channels on the silicon wafer and covering the channels with a Pyrex glass plate. By analyzing the positions of the vapor plug and liquid plug as well as the transient meniscus position, it was found that the liquid transfer from the condensation section to the evaporation section is highly aided by gravity.

Though using oscillating heat pipes partly or wholly made by glass could lead to easier observation of the inner flow patterns, copper or aluminum oscillating heat pipes, which are made by opaque material, are more frequently used in BTMSs during real application. For copper or aluminum oscillating heat pipes, neutron radiography and an infrared technique could be used to realize visualization of inside flow movement during experiments. Perna et al.[77] realized the visualization of the liquid slugs by an infrared technique and calculated the transient flow velocity according to infrared images; they found that both the frequency of pressure signals and oscillating flow velocity increase with the rising heating power. Thompson et al.,[70] Yoon et al.,[78] and Yasuda et al.[79] visualized the transient working fluid distribution by neutron radiography and calculated the liquid volume fraction in the evaporation section; as indicated by their results, no matter whether the heater is placed at the bottom or top side, the working fluid would distribute in the condensation section during operation at high heating power; besides, with the increase of heating power, increases in the oscillation amplitude and oscillating frequency of the liquid slugs will be accompanied.

Besides experiment methods, the visualization of the inside flow pattern can also be realized by numerical methods, such as

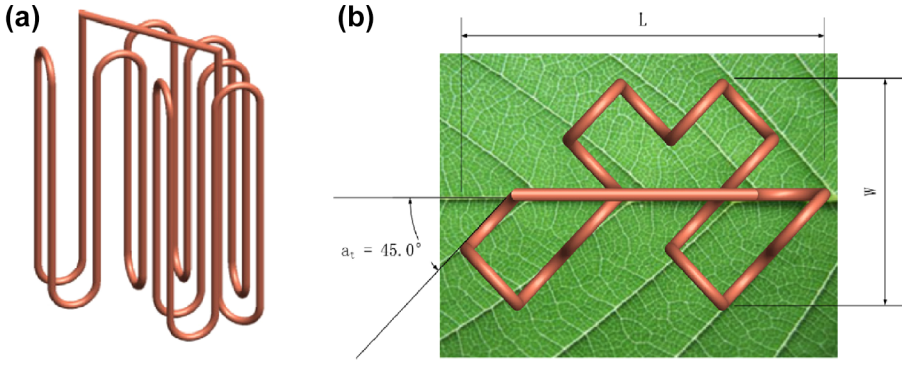

Figure 7. Schematic of a leaf-shaped oscillating heat pipe. Reprinted with permission from ref 59. Copyright 2020 Elsevier.

https://doi.org/10.1021/acsomega.3c08056
ACS Omega 2024, 9, 97−116

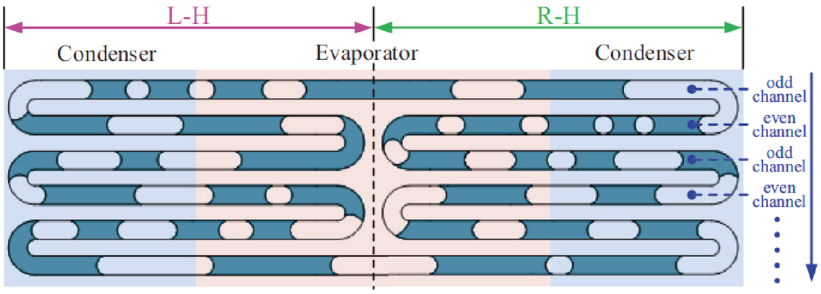

Figure 8. Structure of a dual-serpentine-channel oscillating heat pipe. Reprinted with permission from ref 61. Copyright 2020 Elsevier.

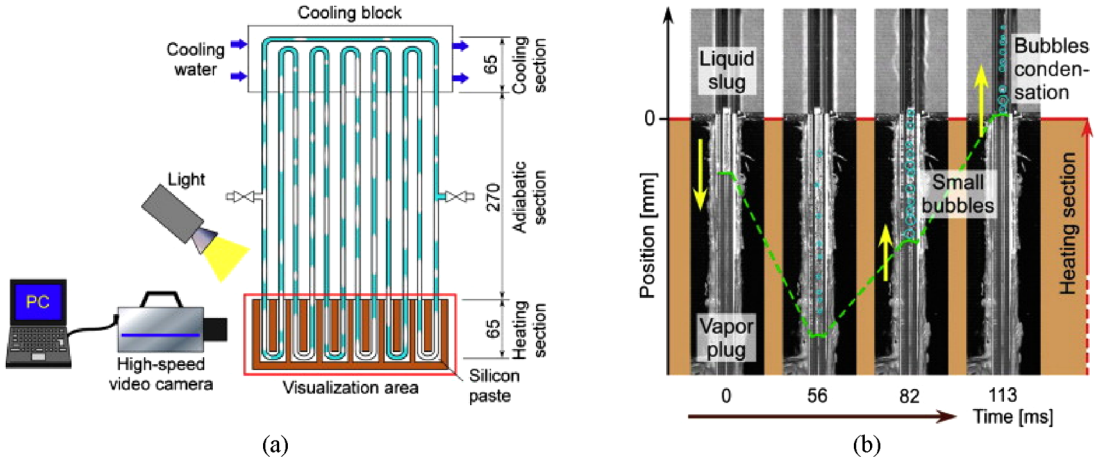

Figure 9. Experiment set up for the visualization of the inside flow pattern of oscillating heat pipe(a) and the image of bubble generation and growth(b). Reprinted with permission from ref 74, Copyright 2013 Elsevier.

simulations based on 1D models, 2D models, and 3D models. Zhao et al.[80] captured the transient pressures of vapor plugs and locations of liquid slugs by a 1D model; they found that the transient movement of the fluid in the oscillating heat pipe is highly associated with heating modes; thus, heating modes should be taken into consideration when designing oscillating heat pipes. Nevertheless, the detailed distribution, length, and shape of all the liquid slugs and vapor plugs could not be accurately described by the 1D model. The spatial distribution of liquid slugs and vapor plugs in the whole oscillating heat pipes could be more clearly captured by 2D or 3D models; however, 2D models are not adaptable to investigations focused on the effects of the cross section geometry of channels and could not be used for the simulation of oscillating heat pipes with 3D structures.[65,81,82] 3D models could be used to simulate oscillating heat pipes with different structures and investigate the effects of different influencing factors, but the computational consumption would be raised significantly.[71]

As could be summarized from the above studies (Table 4), visualization of the flow field inside the oscillating heat pipes has been realized with constant or pulsed heating power and pure liquid as the working fluid. The visualization studies regarding oscillating heat pipes charged by nanofluids and heated by a transient heating cycle have not been conducted yet. In addition, visualization studies of oscillating heat pipes with different structures are still needed.

4. BTMSS BASED ON FLEXIBLE HEAT PIPES

Generally, heat pipes are made of rigid copper tubes due to the high thermal conductivity, which means the shape of the heat pipe could not be changed, which may cause difficulties in the arrangement of the BTMS. Heat pipes made of bendable materials are capable of changing different configurations; thus, they have higher spatial flexibility. Originally, flexible heat pipes were designed for the thermal management of sensors, charge coupled device, or mechanical systems in aerospace field as location change could not be avoided and the arrangement of space is more difficult in a space shuttle or aircraft.[83] Nowadays, flexible heat pipes have been used in land electric devices, such as Li-ion batteries, to meet the demand of space optimization. The investigations of BTMSs based on flexible heat pipes are summarized in Table 5.

4.1. Methods for the Realization of Flexibility. In general, flexibility of heat pipes could be improved by two methods, i.e., using flexible materials as the casing material of the whole heat pipe and using flexible materials as the material of the adiabatic section. However, if the whole or part of the heat pipes are produced from flexible materials, the thermal conductivity would be high, leading to poor cooling performance; thus, flexible materials combined with metal wick structures have become a preferable choice in flexible heat pipes. Oshman et al.,[84−86] Hsieh and Yang,[87] and Liu et al.[92] used liquid crystal polymer with copper filled thermal vias, silicone rubber with copper filled thermal vias, or multilayer polymer/aluminum as the casing material and copper or stainless steel as the material for the wick structure to realize the flexibility of heat pipes; besides, they proved that the thermal conductivity of flexible heat pipe could be significantly higher than copper plate with the same size. For flexible oscillating heat pipes, the wick structure could be omitted; thus, only the materials for the case structure are necessary. However, for polymer-based heat pipes both with and without

https://doi.org/10.1021/acsomega.3c08056
ACS Omega 2024, 9, 97−116

Table 4. Visualization of Inside Flow Movement of BTMSs Based on Oscillating Heat Pipes

Heat source	Heating power	Cooling method	Working fluid	Focus of investigation	Research method	Source
Heating wire	50 W	Natural air cooling	Methanol	Transient fluid movement including nucleation boiling, coalescence of bubbles, wavy flow as well as formation of vapor plugs and liquid slugs.	Experiment	Tong et al. 2001[72]
Rectangular electric heater	0.3−1.2 W/cm^2	Constant temperature water bath	Ethanol/R-142b	Transient fluid movement including the generation and growth of bubbles, the formation of vapor plugs and liquid slugs as well as the movement of capillary slug flow with different numbers of turns.	Experiment	Kim et al. 2003[63]
Heating wire	10 W, 30 W	Natural air cooling	Methanol/water	Transient size distribution and velocity of bubbles.	Experiment	Xu et al. 2005[73]
Electric heating block	0−250 W	Cooling block cooled by constant temperature heavy water	Heavy water	The direction for the movement of liquid slugs and the vapor volume fraction of the whole heat pipe; effects of adding Tesla check valve.	Experiment	Thompson et al. 2011.[70]
Electric strip heater	0−300 W	Cooling plate cooled by constant temperature heavy water	Water	Effects of heating power on temperature distribution and liquid volume fraction in the evaporation section.	Experiment	Yoon et al. 2012[78]
Electric heating block	60 W, 80 W	Cooling plate cooled by constant temperature cooling water	Ethanol	Phase change behavior in the evaporation sector.	Experiment	Senjaya and Inoue 2013[74]
Constant heat flux applied to the evaporation section	10−40 W	Imposed temperature	Water	Transient inside flow pattern; effects of heating power and length ratio between the evaporation section and condensation section.	2D simulation	Wang et al. 2015[65]
Rectangular electric heater	0.5−82 W	Constant temperature water bath/water jacket cooled by constant temperature cooling water	Ethanol/FC-72/R134a	Transient movement of vapor plugs, liquid slugs and meniscus; effects of heating power, number of turns, hydraulic diameter and cross section geometry.	Experiment and simulation based on theoretical model	Kim et al. 2016, 2017, 2020[64,66,75,76]
Imposed heat flux on the boundary/imposed temperature on the boundary	10−65 W	Imposed temperature on the boundary	Water	Effects of heating power and filling ratio.	2D simulation	Pouryoussefi and Zhang 2016, 2017[81,82]
Heating wire	38−110 W	Forced air convection	Ethanol	Effects of filling ratio and heating power on transient bubble displacement, bubble velocity and bubble size distribution.	Experiment	Sun et al. 2017[68]
Two electric heating elements	68−146 W	Cooling plate cooled by constant temperature cooling water	Fluorinert electronic liquid (FC-72)	Transient infrared images and effects of heating power.	Experiment	Perna et al. 2020[77]
Imposed heat flux on the boundary	66.5−161.9 W	Imposed temperature on the boundary	Working fluid with latent heat of 7.12×10^5 J/g and kinematic viscosity of 5.01×10^{-7} m^2/s	Effects of heating modes on heat transfer characteristics, location of liquid slugs and pressure of vapor plugs.	1D simulation	Zhao et al. 2020[80]
Eleven $LiNiCoAlO_2$ battery packs with capacity of 29A·h	Discharge rate from 1.0C to 2.0C	Natural air cooling/forced air cooling/cooling plate cooled by constant temperature cooling water	Water/ethanol	Effects of battery discharge rate, structure of oscillating heat pipe, cooling method and working fluid.	3D simulation	Liu et al. 2021[71]
Imposed temperature on the boundary	Heated by constant temperature of 57 °C	Imposed temperature on the boundary	Water	Effects of the position of separating wall inside the oscillating heat pipe and filling ratio on liquid distribution and heat transfer characteristics.	2D simulation	Kang et al. 2021[69]
Three electric heating block	0−160 W	Cooling plate cooled by constant temperature cooling water	R1336mzz	Visualization of the transient inside flow movement; effects of heating power and location of the heating block.	Experiment	Yasuda et al. 2022[79]

https://doi.org/10.1021/acsomega.3c08056
ACS Omega 2024, 9, 97−116

Table 5. Investigations of BTMSs Based on Flexible Heat Pipes

Heat source	Heating power	Cooling method	Working fluid	Material	Focus of investigation	Research method	Source
Rectangular electric heater	2.9−40 W	Constant temperature water bath/ Cooling plate with circulating cooling water	Water	Liquid crystal polymer(case)+copper(wick structure)	Effects of heating power, inclination angle and acceleration.	Experiment	Oshman et al. 2011, 2012[84,85]
Rectangular electric heater	5−30 W	Cooling plate with circulating cooling water	Water	Polyethylene/aluminum/linear low-density polyethylene terephthalate(case)+ copper(wick structure)+ nylon woven(vapor core)	Effects of heating power and bending angle.	Experiment	Oshman et al. 2013[86]
Rectangular electric heater	6−12.7 W	Constant temperature water bath	Deionized water	Silicone rubber(case)+ copper(wick structure)	Effects of heating power and bending angle.	Experiment	Hsieh and Yang 2013[87]
Silicone rubber heater	2−40 W	Cooling plate with circulating cooling water	Deionized water	Copper(evaporation section and condensation section)+ fluororubber(adiabatic section)	Effects of bending angle and filling ratio.	Experiment	Yang et al. 2016[88]
Rectangular electric heater	4−195 W	Forced air convection	Deionized water	Copper(evaporation section and condensation section)+ fluororubber(adiabatic section)	Effects of filling ratio, configuration and length of adiabatic section.	Experiment	Qu et al. 2017, 2018[89,90]
Film heating sheet	2−16 W	Water jacket with circulating cooling water	HFE-7000	Polyethylene terephthalate/aluminum/linear low-density polyethylene terephthalate(case)+ low density polyethylene(channeled region)	Effects of inclination angle, bending angle and indium coating on the heat-sealed flanges.	Experiment	Lim and Kim 2018[91]
Film heating sheet	4−12 W	Cooling plate with circulating cooling water	Deionized water	Aluminum/cholorinated polypropylene(case)+stainless steel with Fe_2O_3 nanowires(wick structure)	Effects of filling ratio and bending angle.	Experiment	Liu et al. 2019[92]
Rectangular electric heater	6−14 W	Forced air convection	Deionized water	Copper(evaporation section and condensation section)+ copper/polymer(adiabatic section)	Effects of filling ratio and bending angle.	Experiment	Huang et al. 2020[93]
Film heating sheet	3−26 W	Cooling plate with circulating cooling water	HFE-7000	Polyimide/copper(case)+ polycarbonate(channeled region)	Effects of heating power and bending angle.	Experiment	Jung et al. 2020[94]
Rectangular electric heater	5−25 W	Forced air convection	Deionized water	Copper(evaporation section and condensation section)+ polyurethane(adiabatic section)	Effects of heating power, filling ratio, bending angle and inclination angle.	Experiment	Huang et al. 2021[95]

https://doi.org/10.1021/acsomega.3c08056
ACS Omega 2024, 9, 97−116

wick structure, the problem of noncondensable gas permeation from ambient and leakage of working fluid are big issues for the long-term application. These issues could be partly resolved by adding indium coating to aid the sealing of flanges and could be well resolved by using copper-foil or other metallic material as the innermost layer of the case material.[91,94]

Yang et al.,[88] Qu et al.,[89,90] and Huang et al.[93,95] used evaporation and condensation sections made of copper along with adiabatic sections made of rubber tube (Figure 10) or

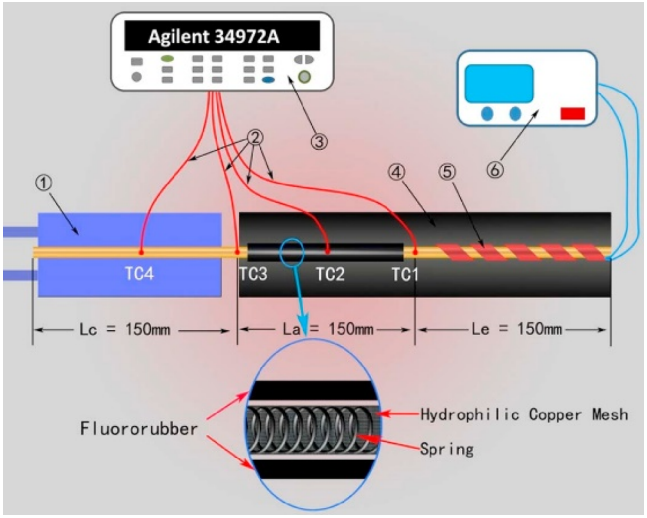

Figure 10. Structure of flexible heat pipe with rubber adiabatic section. Reprinted with permission from ref 88. Copyright 2016 Elsevier.

several copper tubes stuck to a continuous flexible polymer shell to realize the creation of flexible heat pipes. Using these methods to realize flexibility, better thermal conductivity could be achieved as metallic material is adopted for the evaporation and condensation sections. However, the sealing problem between the flexible materials and the metallic materials still exists and could prevent the use of flexible heat pipes with these structures in commercial applications.

4.2. Effects of Bending Angle and Configuration. Working with different bending angles and configurations is inevitable for flexible heat pipes; thus, investigations for the effects of bending angle and configuration are involved in most of the studies regarding flexible heat pipes. As indicated by the results of Oshman et al.,[86] Hsieh and Yang,[87] Lim and Kim,[91,94] and Liu et al.,[92] if the flexible heat pipe is horizontally placed, bending the adiabatic section to make the evaporation section upward would lead to increased thermal resistance while bending the adiabatic section to make the condensation section upward with a small angle (e.g., 15°) could improve the cooling performance. Besides, if the flexible heat pipe is vertically placed and the evaporation section is below the condensation section, bending the adiabatic section to make the condensation section downward or make the evaporation section upward would lead to impaired cooling performance.[88,91,93−95] Generally, bending the flexible heat pipes would lead to increased flow resistance and decreased thermal conductivity; however, if the evaporation section becomes much lower than the condensation section after bending, the beneficial effects of gravity would be more significant, and subsequently, the cooling performance could be improved. In views of configuration, Qu et al.[89,90] investigated the cooling performance of a flexible heat pipe with different configurations (Figure 11). As indicated by their results, the bending

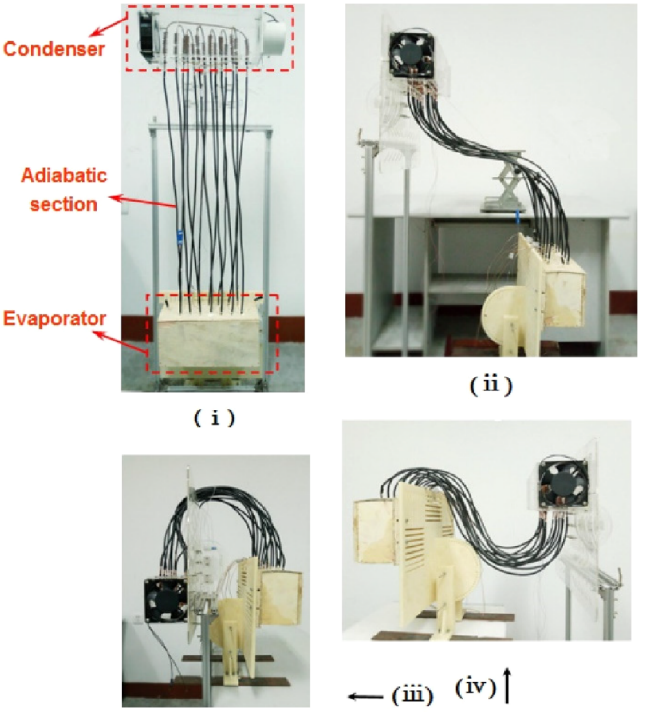

Figure 11. Photo of different configurations of flexible heat pipe: (i) I shape, (ii) stair-step shape, (iii) inverted-U shape, and (iv) N shape. Reprinted with permission from ref 89. Copyright 2017 Elsevier.

of the adiabatic section would lead to increased flow resistance and the subsequent thermal resistance; in this case, the cooling performance of the "I" shape flexible heat pipe is the best while that of the "N" shape is the worst owing to the negative effects of two bendings. For configurations with one bending ("stair-step" shape and "inverted-U" shape), the cooling performance of the inverted-U shape is worse due to the elimination of the positive effects of gravity.

5. BTMSS BASED ON MICROCHANNEL HEAT PIPES

Microchannel heat pipes, i.e., also known as micro heat pipe arrays (MHPA), have an array of multiple parallel channels in them and could be adapted to ultrathin structures. Microchanneled heat pipes are superior to flat single-channel heat pipes with respect to heat transfer efficiency, cooling uniformity, and reliability and, thus, have gained more attention in recent years (Table 6).

5.1. Effects of Cooling Method. Zhao et al.,[96] Liu et al.,[97,98] Ye et al.,[99,100] Dan et al.[101], and Mo et al.[102] adopted microchannel heat pipes in BTMSs and compared the cooling performance of different cooling methods. According to their results, at high discharge rates, using BTMSs with a microchanneled heat pipe combined with natural convection could not realize acceptable cooling performance. Better cooling performance could be achieved by using forced air convection or water cooling, while when water bath cooling is applied, reduced thermal conductivity compared to forced air convection may be induced by unstable transitional film boiling. The best cooling method seems to be microchanneled heat pipe combined with water spray, and this cooling method was proven to meet the cooling requirements with respect to

https://doi.org/10.1021/acsomega.3c08056
ACS Omega 2024, 9, 97−116

Table 6. Investigations of BTMSs Based on Microchannel Heat Pipes

Battery type	Nominal Capacity per cell	Nominal voltage per cell	Cooling method	Working fluid	Focus of investigation	Research method	Source
Li-ion battery pack with 4 pouch cells	3 A·h/8 A·h	3.7 V	Natural/forced air cooling; water cooling(thermostat bath and water spray)	Acetone	Effects of discharge rate and cooling method.	Experiment	Zhao et al. 2015[96]
Li-ion battery pack with 5 prismatic cells	50 A·h	3.2 V	Natural/forced air cooling	Water	Effects of discharge rate, cooling method and heating method.	Experiment and 3D simulation	Liu et al. 2016, 2018[97,98]
$LiFePO_4$ battery module with 16 prismatic cells	18 A·h	3.2 V	Natural/forced air cooling		Effects of discharge rate, cooling method and inclination angle.	Experiment	Ye et al. 2018[99,100]
Li-ion battery module with 96 prismatic cells	55 A·h	3.2 V	Natural/forced air cooling	Acetone	Effects of discharge rate, cooling method and cooling air velocity.	Simulation based on theoretical model	Dan et al. 2019[101]
$LiFePO_4$ battery module with 12 pouch cells	28 A·h		Forced air cooling/cooling block with circulating cooling water		Effects of discharge rate and cooling method.	Experiment and 3D simulation	Mo et al. 2019[102]
Battery simulator(two silicone heaters)			Cooling plate with circulating cooling water	Water	Effects of cooling water velocity.	Simulation based on theoretical model	Guichet et al. 2020[103]
Li-ion battery module with 6 prismatic cells	120 A·h	3.2 V	Natural/forced air cooling		Effects of charge/discharge rate and cooling method.	Experiment	Ren et al. 2021[104]
$Li(NixCoyMnz)O_2$ battery module with 12 prismatic cells	50 A·h	3.6 V	Cooling plate with circulating cooling water		Effects of charge/discharge rate and ambient temperature.	Experiment	Liang et al. 2021[105]
$Li(NixCoyMnz)O_2$ battery pack with 5 prismatic cells	15 A·h	3.65 V	Natural air cooling/forced air cooling/water spray		Effects of discharge rate, cooling method and cooling air velocity.	Experiment	Yue et al. 2021[106]
$LiFePO_4$ battery pack with 2/8/16 cells	18 A·h	3.2 V	Natural air cooling	Acetone	Effects of heating power and ambient temperature.	Experiment and 3D simulation	Wang et al. 2021[107]
$LiFePO_4$ battery pack with 12 cells	52 A·h	3.13 V	Water cooling		Effects of ambient temperature and insulation shell.	Experiment	Liang et al. 2023[108]

https://doi.org/10.1021/acsomega.3c08056
ACS Omega 2024, 9, 97−116

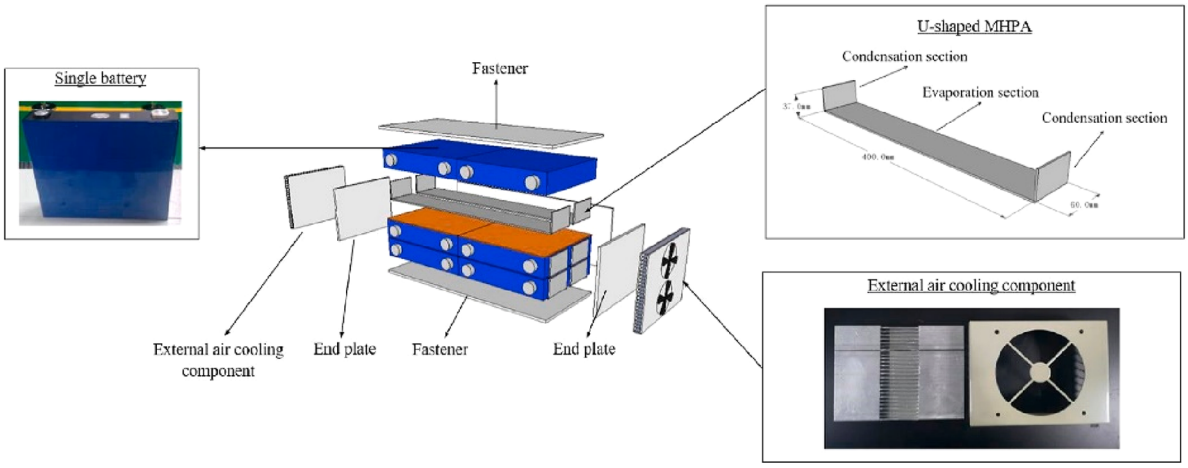

Figure 12. Configuration of U-shaped microchannel heat pipe. Reprinted with permission from ref 104. Copyright 2021 Elsevier.

temperature rise and temperature uniformity. When water spray is used with the aid of forced air convection, the cooling performance could be further improved; meanwhile, the energy consumption is much less than that of pure forced air convection.[106]

5.2. Effects of Other Factors. The effects of cooing air velocity, cooling water velocity, and inclination angle on the cooling performance of microchannel heat pipes are similar to those of flat single-channel heat pipes, i.e., increasing cooling air/water velocity or lifting the condensation section up could improve the heat transfer characteristics.[103] Generally, microchannel heat pipes are featured by a flat plate structure; however, when a U-shaped microchannel heat pipe is adopted instead of a flat plate microchannel heat pipe (Figure 12), smaller temperature rise could be obtained with sacrifices in temperature uniformity. Though temperature differences would be enlarged with the application of U-shaped microchannel heat pipe, the temperature differences within a cell or a module could be maintained below 5 °C at high discharge rates when forced air convection or cooling plate with circulating cooling water is used.[104,105] In addition, it should be noted that low-temperature operation is inevitable for the Li-ion battery, and the heating performance is also important for BTMSs. However, most studies concerning BTMSs based heat pipes are focused on cooling performance rather than heating performance, and Wang et al.[107] pointed out that the equipment of microchannel heat pipes have negative effects on temperature rise. To improve the heating performance under low-temperature conditions, Liang et al.[108] designed bending (Z-shape) flat micro heat pipe array and systemically explored the preheating performance of BTMS based bending flat micro heat pipe array; as indicated by their results, temperature rise rate can reach about 1 °C/min at ambient temperatures of −20 °C, −10 °C, and 0 °C with temperature differences within 5 °C. However, the related research is still rare and heating performance should be considered for all types of BTMSs based on heat pipes.

6. CONCLUSIONS AND PROSPECTS

6.1. Conclusions. (1) For all types of BTMSs based on heat pipes, the cooling method exerted on the condensation section has great impacts on heat transfer behavior and cooling performance. Generally, natural air convection could not control the temperature rise and temperature difference within the acceptable range for high-power Li-ion batteries. Using forced air convection, water bath cooling or water cooling plate could improve the cooling performance of BTMSs based on heat pipes; however, the control of cooling charge mass flow rate (or velocity) is a key issue.

(2) For BTMSs based on oscillating heat pipes, improved heat transfer characteristics could be achieved by increasing number of turns, using relatively larger inner hydraulic diameter and using length ratio between the evaporator and condenser higher than 1.0. It was also found that the choice of working fluid is highly dependent on the material of oscillating heat pipes.

(3) If the basic geometry parameters, working fluid, and filling ratio are optimized, the cooling performance of BTMSs based on oscillating heat pipes could be further improved by adding PCM or designing new structures, such as 3D structures, dual-serpentine-channel, channels with Tesla valves etc. It was also pointed out that adding separating walls in the capillary channels has beneficial effects on the cooling performance, whereas the location of the separating walls should be carefully designed to obtain optimum cooling performance.

(4) Visualization of BTMSs based on oscillating heat pipes could be realized by fabricating the oscillating heat pipes by transparent material (e.g., Pyrex glass) in whole or part. For oscillating heat pipes fabricated by opaque material (e.g., copper and aluminum), infrared technique or neutron radiography could be adopted for the investigation of detailed inside flow patterns.

(5) Flexibility of BTMSs based on heat pipes could be realized by using flexible material as the case material or changing the material of adiabatic section from rigid material to flexible material. However, compared to metallic materials, flexible materials have lower thermal conductivity; meanwhile, oscillating heat pipes fabricated by flexible materials suffer from permeation of noncondensable gases from ambient and leakage of working fluid. These issues could be partly resolved by adding thermal vias filled with metallic materials and covering the sealing part with indium coating or designing multilayered structure with metallic materials in it.

(6) BTMSs based on microchannel heat pipes could achieve better cooling performance than flat single-channel heat pipes with the same size if appropriately designed. The effects of cooling methods, cooling charge velocity, and inclination angle

https://doi.org/10.1021/acsomega.3c08056
ACS Omega 2024, 9, 97−116

on the cooling performance on microchannel heat pipes are similar to those on flat single-channel heat pipes.

6.2. Limitations and Prospects. (1) It is concluded that water spray cooling is an effective and energy saving cooling method. However, detailed investigations focused on the combined use of heat pipes and water spray cooling are still rare. Studies regarding the effects of the injection frequency, injection mass flow rate, and injector parameters of water spray cooling system equipped on BTMSs based heat pipes should be conducted in the future.

(2) For Li-ion batteries, it is important to prevent the propagation of thermal runaway. However, only a few studies have been performed to explore the thermal runaway behavior of BTMSs based on flat single-channel heat pipes. The effects of other heat pipes on the thermal runaway behavior of Li-ion batteries have not been systematically clarified yet.

(3) For BTMSs based on oscillating heat pipes, the nanofluids adopted have been proven to have the capability of heat transfer improvement. However, the operation stability and heat transfer characteristics in the long-run have not been systematically studied for BTMSs based on oscillating heat pipes charged with nanofluids. Additionally, visualization investigations on BTMSs based on oscillating heat pipes charged with nanofluids are essential to clarify the inside flow pattern and the movement of the nanoadditives.

(4) In view of BTMSs based on flexible heat pipes, the issues of low thermal conductivity, working fluid leakage and permeation of noncondensable gases from ambient have been pointed out. However, the long-term cooling performance of BTMSs based on different flexible heat pipes has not been thoroughly investigated. In this case, comparisons between the cooling performance and long-term reliability between flexible heat pipes fabricated by different flexible materials could be a future research focus. Besides, for flexible heat pipes with rigid evaporator and condenser as well as a bendable adiabatic section, efforts to solve the sealing issue between the metallic part and the flexible part are required.

(5) It is pointed out that the design and geometry parameters of the BTMSs based on heat pipes have significant effect on their heat transfer characteristics and cooling performance. Meanwhile, the optimizations for the structure and geometry parameters are more meaningful when the BTMSs based on heat pipes are equipped on real batteries rather than electric heaters. From this point of view, studies regarding the performance of new structures and the effects of geometry parameters are still needed for different heat pipes used in BTMSs.

(6) As heat pipes demonstrate superior cooling performance, the studies regarding BTMSs based on heat pipes are concentrated on their cooling performance. However, when operating at low temperatures, the heating performance of BTMSs becomes a key issue. Hence, the effects of heating method on the heat pipe based BTMSs and the evaluation of the heating performance of BTMSs based different heat pipes should be regarded as future research interests.

(7) For all types of BTMSs based on heat pipes, additional cooling methods are needed for efficient battery cooling, which may increase space occupation. Moreover, raised maintenance complexity and manufacturing cost are inevitable when heat pipes are adopted, which further limits their commercial use in BTMSs.

(8) As indicated by the study of Ginting et al.,[109] the performance of heat pipes could be significantly influenced by inner surface treatment. Superhydrophilic surface modification to the inner surface could enhance the cooling performance of heat pipe. However, studies focused on the application of surface modified heat pipes to BTMSs are rare. Thereby, such studies are still needed.

AUTHOR INFORMATION

Corresponding Authors

Xin Liu − *Systems Engineering Institute, AMS, PLA, Tianjin 300161, China*; orcid.org/0009-0008-4673-5682; Email: wqsliuxin@126.com

Zhenguo Li − *China Automotive Technology & Research Center, Co., Ltd., Tianjin 300300, China; CATARC Automotive Test Center (Tianjin) Co., Ltd., Tianjin 300300, China*; Email: zgli_catarc@sina.com

Authors

Hanming Wu − *China Automotive Technology & Research Center, Co., Ltd., Tianjin 300300, China; CATARC Automotive Test Center (Tianjin) Co., Ltd., Tianjin 300300, China*

Ming Niu − *School of Energy and Environmental Engineering, Hebei University of Technology, Tianjin 300401, China*

Yuankai Shao − *China Automotive Technology & Research Center, Co., Ltd., Tianjin 300300, China; CATARC Automotive Test Center (Tianjin) Co., Ltd., Tianjin 300300, China*

Maoxuan Wang − *China Automotive Technology & Research Center, Co., Ltd., Tianjin 300300, China; CATARC Automotive Test Center (Tianjin) Co., Ltd., Tianjin 300300, China*

Menghan Li − *School of Energy and Environmental Engineering, Hebei University of Technology, Tianjin 300401, China*

Complete contact information is available at: https://pubs.acs.org/10.1021/acsomega.3c08056

Notes

The authors declare no competing financial interest.

ACKNOWLEDGMENTS

This work was supported by the Ministry of Science and Technology of the People's Republic of China (No.2022YFE0207900).

NOMENCLATURE

T_e	temperature of evaporation section
T_{sat}	saturation temperature
T_c	temperature of condensation section

SUBSCRIPTS

e	evaporation section
sat	saturation
c	condensation section

Acronyms

1D	one-dimensional
2D	two-dimensional
3D	three-dimensional
BTMS	battery thermal management system
EV	electric vehicle
EG	expanded graphite
HEV	hybrid electric vehicle

https://doi.org/10.1021/acsomega.3c08056
ACS Omega 2024, 9, 97−116

MHPA micro heat pipe array
OHP oscillating heat pipe
PCM phase change material
SOC state of charge

REFERENCES

(1) Lan, X.; Tans, P.; Thoning, K. W. *Trends in globally-averaged CO2 determined from NOAA Global Monitoring Laboratory measurements*; NOAA/GML, 2023-12. https://gml.noaa.gov/ccgg/trends/gl_data.html (accessed 12/24/2023).

(2) British Petroleum. Energy Outlook, https://www.bp.com/en/global/corporate/energy-economics/energy-outlook (accessed 12/24/2023).

(3) Duh, Y. S.; Sun, Y. J.; Lin, X.; Zheng, J. J.; Wang, M. C.; Wang, Y. J.; Lin, X. Y.; Jiang, X. Y.; Zheng, Z. G.; Zheng, S.; Yu, G. Characterization on thermal runaway of commercial 18650 lithium-ion batteries used in electric vehicles: A review. *Journal of Energy Storage* **2021**, *41*, No. 102888.

(4) Chen, J.; Manivanan, M.; Duque, J.; Kollmeyer, P.; Panchal, S.; Gross, O.; Emadi, A. A convolutional neural network for estimation of lithium-ion battery state-of-health during constant current operation. 2023 *IEEE Transportation Electrification Conference & Expo(ITEC)*, Detroit, United States, June 21−23, 2023.

(5) Abada, S.; Marlair, G.; Lecocq, A.; Petit, M.; Sauvant-Moynot, V.; Huet, F. Safety focused modeling of lithium-ion batteries: A review. *J. Power Sources* **2016**, *306*, 178−192.

(6) Vashisht, S.; Rakshit, D.; Panchal, S.; Fowler, M.; Fraser, R. Thermal behaviour of Li-ion battery: An improved electrothermal model considering the effects of depth of discharge and temperature. *Journal of Energy Storage* **2023**, *70*, No. 107797.

(7) Baveja, R.; Bhattacharya, J.; Panchal, S.; Fraser, R.; Fowler, M. Predicting temperature distribution of passively balanced battery module under realistic driving conditions through coupled equivalent circuit method and lumped heat dissipation method. *Journal of Energy Storage* **2023**, *70*, No. 107967.

(8) Yang, R.; Xie, Y.; Li, K.; Tran, M. K.; Fowler, M.; Panchal, S.; Deng, Z.; Zhang, Y. Comparative study on the thermal characteristics of solid-state lithium-ion batteries. *IEEE Transactions on Transportation Electrification* **2023**, 1.

(9) Arora, S. Selection of thermal management system for modular battery packs of electric vehicles: A review of existing and emerging technologies. *J. Power Sources* **2018**, *400*, 621−640.

(10) Liu, Z. Y.; Wang, H.; Yang, C.; Zhao, J. J. Simulation study of lithium-ion battery thermal management system based on a variable flow velocity method with liquid metal. *Applied Thermal Engineering* **2020**, *179*, No. 115578.

(11) Talele, V.; Moralı, U.; Patil, M. S.; Panchal, S.; Fraser, R.; Fowler, M.; Thorat, P.; Gokhale, Y. P. Computational modelling and statistical evaluation of thermal runaway safety regime response on lithium-ion battery with different cathodic chemistry and varying ambient condition. *International Communications in Heat and Mass Transfer* **2023**, *146*, No. 106907.

(12) Zhao, G.; Wang, X. L.; Negnevitsky, M.; Zhang, H. Y. A review of air-cooling battery thermal management systems for electric and hybrid electric vehicles. *J. Power Sources* **2021**, *501*, No. 230001.

(13) Subhedar, D.; Chauhan, K. V.; Panchal, S.; Bais, A. Numerical investigation of performance for liquid-cooled cylindrical electrical vehicle battery pack using Al2O3/EG-water nano coolant. *Materials Today: Proceedings* **2023**, 1 DOI: 10.1016/j.matpr.2023.08.055.

(14) Akbarzadeh, M.; Kalogiannis, T.; Jaguemont, J.; Jin, L.; Behi, H.; Karimi, D.; Beheshti, H.; Mierlo, J. V.; Berecibar, M. A comparative study between air cooling and liquid cooling thermal management systems for a high-energy lithium-ion battery module. *Applied Thermal Engineering* **2021**, *198*, No. 117503.

(15) Rao, Z. H.; Wang, S. F.; Zhang, G. Q. Simulation and experiment of thermal energy management with phase change material for ageing LiFePO4 power battery. *Energy Conversion and Management* **2011**, *52*, 3408−3414.

(16) Kausthubharam; Koorata, P. K.; Panchal, S. Thermal management of large-sized LiFePO4 pouch cell using simplified mini-channel cold plates. *Applied Thermal Engineering* **2023**, *234*, No. 121286.

(17) Bais, A.; Subhedar, D.; Panchal, S. Experimental investigation of longevity and temperature of a lithium-ion battery cell using phase change material based battery thermal management system. *Materials Today: Proceedings* **2023**, 1 DOI: 10.1016/j.matpr.2023.08.103.

(18) Joshi, A. K.; Kakati, P.; Dandotiya, D.; Prashanth, S. P.; Patil, N. G.; Panchal, S. Computational Analysis of Preheating Cylindrical Lithium-Ion Batteries with Fin-Assisted Phase Change Material-(PCM). *International Journal of Modern Physics C* **2023**, 1 DOI: 10.1142/S0129183124500475.

(19) Wu, W. X.; Wang, S. F.; Wu, W.; Chen, K.; Hong, S. H.; Lai, Y. X. A critical review of battery thermal performance and liquid based battery thermal management. *Energy Conversion and Management* **2019**, *182*, 262−281.

(20) Lin, C. J.; Xu, S. C.; Chang, G. F.; Liu, J. L. Experiment and simulation of a LiFePO4 battery pack with a passive thermal management system using composite phase change material and graphite sheets. *J. Power Sources* **2015**, *275*, 742−749.

(21) Jiang, G. W.; Huang, J. H.; Liu, M. C.; Cao, M. Experiment and simulation of thermal management for a tube-shell Li-ion battery pack with composite phase change material. *Applied Thermal Engineering* **2017**, *120*, 1−9.

(22) Liu, F.; Wang, J. F.; Liu, Y. Q.; Wang, F. Q.; Yang, N.; Liu, X. D.; Liu, H.; Li, W. X.; Liu, H. T.; Huang, B. Performance analysis of phase change material in battery thermal management with biomimetic honeycomb fin. *Applied Thermal Engineering* **2021**, *196*, No. 117296.

(23) Alihosseini, A.; Shafaee, M. Experimental study and numerical simulation of a lithium-ion battery thermal management system using a heat pipe. *Journal of Energy Storage* **2021**, *39*, No. 102616.

(24) Rao, Z. H.; Wang, S. F.; Wu, M. C.; Lin, Z. R.; Li, F. H. Experimental investigation on thermal management of electric vehicle battery with heat pipe. *Energy Conversion and Management* **2013**, *65*, 92−97.

(25) Tran, T.-H.; Harmand, S.; Desmet, B.; Filangi, S. Experimental investigation on the feasibility of heat pipe cooling for HEV/EV lithium-ion battery. *Applied Thermal Engineering* **2014**, *63*, 551−558.

(26) Ye, Y. H.; Saw, L. H.; Shi, Y. X.; Tay, A. A. O. Numerical analyses on optimizing a heat pipe thermal management system for lithium-ion batteries during fast charging. *Applied Thermal Engineering* **2015**, *86*, 281−291.

(27) Wang, Q.; Jiang, B.; Xue, Q. F.; Sun, H. L.; Li, B.; Zou, H. M.; Yan, Y. Y. Experimental investigation on EV battery cooling and heating by heat pipes. *Applied Thermal Engineering* **2015**, *88*, 54−60.

(28) Wu, W. X.; Yang, X. Q.; Zhang, G. Q.; Chen, K.; Wang, S. F. Experimental investigation on the thermal performance of heat pipe-assisted phase change material based battery thermal management system. *Energy Conversion and Management* **2017**, *138*, 486−492.

(29) Wang, S. Q.; Lu, L. G.; Ren, D. S.; Feng, X. N.; Gao, S.; Ouyang, M. G. Experimental investigation on the feasibility of heat pipe-based thermal management system to prevent thermal runaway propagation. *Journal of Electrochemical Energy Conversion and Storage* **2019**, *16*, No. 031006.

(30) Li, Y.; Qi, F.; Guo, H.; Guo, Z. P.; Xu, G.; Liu, J. Numerical investigation of thermal runaway propagation in a Li-ion battery module using the heat pipe cooling system. *Numerical Heat Transfer, Part A: Applications* **2019**, *75* (3), 183−199.

(31) Xu, X. M.; Tang, W.; Fu, J. Q.; Li, R. Z.; Sun, X. Plate flat heat pipe and liquid-cooled coupled multistage heat dissipation system of Li-ion battery. *International Journal of Energy Research* **2019**, *43* (3), 1133−1141.

(32) Zhang, Z. Q.; Wei, K. Experimental and numerical study of a passive thermal management system using flat heat pipes for lithium-ion batteries. *Applied Thermal Engineering* **2020**, *166*, No. 114660.

(33) Zhang, W. C.; Liang, Z. C.; Wu, W. X.; Ling, G. Z.; Ma, R. X. Design and optimization of a hybrid battery thermal management

https://doi.org/10.1021/acsomega.3c08056
ACS Omega 2024, 9, 97−116

system for electric vehicle based on surrogate model. *Int. J. Heat Mass Transfer* **2021**, *174*, No. 121318.
(34) Liang, Z.; Wang, R.; Malt, A. H.; Souri, M.; Esfahani, M.N.; Jabbari, M. Systematic evaluation of a flat-heat-pipe-based thermal management: Cell-to-cell variations and battery ageing. *Applied Thermal Engineering* **2021**, *192*, No. 116934.
(35) Abbas, S.; Ramadan, Z.; Park, C. W. Thermal performance analysis of compact-type simulative battery module with paraffin as phase-change material and flat plate heat pipe. *Int. J. Heat Mass Transfer* **2021**, *173*, No. 121269.
(36) Tang, Z. Y.; Feng, R. L.; Huang, P. F.; Bai, Z. H.; Wang, Q. S. Modeling analysis on the cooling efficiency of composite phase change material-heat pipe coupling system in battery pack. *Journal of Loss Prevention in the Process Industries* **2022**, *78*, No. 104829.
(37) Jang, D. S.; Ham, S. H.; Kim, J. Y.; Kim, Y. C. Thermal and aging performance characteristics of pouch-type lithium-ion battery using heat pipes under nonuniform heating conditions. *Applied Thermal Engineering* **2024**, *236*, No. 121891.
(38) Singh, B.; Kumar, P. Heat transfer enhancement in pulsating heat pipe by alcohol-water based self-rewetting fluid. *Thermal Science and Engineering Progress* **2021**, *22*, No. 100809.
(39) Zhang, X. M.; Xu, J. L.; Zhou, Z. Q. Experimental study of a pulsating heat pipe FC-72, ethanol and water as working fluids. *Experiment Heat Transfer* **2004**, *17*, 47−67.
(40) Rittidech, S.; Pipatpaiboon, N.; Terdtoon, P. Heat-transfer characteristics of a closed-loop oscillating heat-pipe with check valves. *Applied Energy* **2007**, *84*, 565−577.
(41) Qu, W.; Ma, H. B. Theoretical analysis of startup of a pulsating heat pipe. *Int. J. Heat Mass Transfer* **2007**, *50*, 2309−2316.
(42) Lin, Z. R.; Wang, S. F.; Chen, J. J.; Huo, J. P.; Hu, Y. X.; Zhang, W. Experimental study on effective range of miniature oscillating heat pipes. *Applied Thermal Engineering* **2011**, *31*, 880−886.
(43) Zhu, Y.; Cui, X. Y.; Han, H.; Sun, S. D. The study on the difference of the start-up and heat-transfer performance of the pulsating heat pipe with water-acetone mixtures. *Int. J. Heat Mass Transfer* **2014**, *77*, 834−842.
(44) Rao, Z. H.; Huo, Y. T.; Liu, X. J. Experimental study of an OHP-cooled thermal management system for electric vehicle power battery. *Experimental Thermal and Fluid Science* **2014**, *57*, 20−26.
(45) Hu, Y. X.; Liu, T. Q.; Li, X. Y.; Wang, S. F. Heat transfer enhancement of micro oscillating heat pipes with self-rewetting fluid. *Int. J. Heat Mass Transfer* **2014**, *70*, 496−503.
(46) Goshayeshi, H. R.; Goodarzi, M.; Dahari, M. Effect of magnetic field on the heat transfer rate of kerosene/Fe2O3 nanofluid in a copper oscillating heat pipe. *Experimental Thermal and Fluid Science* **2015**, *68*, 663−668.
(47) Su, X. J.; Zhang, M.; Han, W.; Guo, X. M. Experimental study on the heat transfer performance of an oscillating heat pipe with self-rewetting nanofluid. *Int. J. Heat Mass Transfer* **2016**, *100*, 378−385.
(48) Wang, Q. C.; Rao, Z. H.; Huo, Y. T.; Wang, S. F. Thermal performance of phase change material/oscillating heat pipe-based battery thermal management system. *International Journal of Thermal Sciences* **2016**, *102*, 9−16.
(49) Rao, Z. H.; Wang, Q. C.; Zhao, J. T.; Huang, C. L. Experimental investigation on the thermal performance of a closed oscillating heat pipe in thermal management. *Heat and Mass Transfer* **2017**, *53*, 3059−3071.
(50) Zhao, J. T.; Qu, J.; Rao, Z. H. Thermal characteristic and analysis of closed loop oscillation heat pipe/phase change material (CLOHP/PCM) coupling module with different working media. *Int. J. Heat Mass Transfer* **2018**, *126*, 257−266.
(51) Jang, D. S.; Chung, H. J.; Jeon, Y.; Kim, Y. C. Thermal performance characteristics of a pulsating heat pipe at various non-uniform heating conditions. *Int. J. Heat Mass Transfer* **2018**, *126*, 855−863.
(52) Chi, R. G.; Chung, W. S.; Rhi, S. H. Thermal characteristics of an oscillating heat pipe cooling system for electric vehicle Li-Ion batteries. *Energies* **2018**, *11*, 655.
(53) Qu, J.; Ke, Z. Q.; Zuo, A. H.; Rao, Z. H. Experimental investigation on thermal performance of phase change material coupled with three-dimensional oscillating heat pipe (PCM/3DOHP) for thermal management application. *Int. J. Heat Mass Transfer* **2019**, *129*, 773−782.
(54) Hao, T. T.; Ma, H. B.; Ma, X. H. Heat transfer performance of polytetrafluoroethylene oscillating heat pipe with water, ethanol and acetone as working fluids. *Int. J. Heat Mass Transfer* **2019**, *131*, 109−120.
(55) Wei, A. B.; Qu, J.; Qiu, H. H.; Wang, C.; Cao, G. H. Heat transfer characteristics of plug-in oscillating heat pipe with binary-fluid mixtures for electric vehicle battery thermal management. *Int. J. Heat Mass Transfer* **2019**, *135*, 746−750.
(56) Chi, R. G.; Rhi, S. H. Oscillating heat pipe cooling system of electric vehicle's Li-ion batteries with direct contact bottom cooling mode. *Energies* **2019**, *12*, 1698.
(57) Xu, Y. Y.; Xue, Y. Q.; Qi, H.; Cai, W. H. Experimental study on heat transfer performance of pulsating heat pipes with hybrid working fluids. *Int. J. Heat Mass Transfer* **2020**, *157*, No. 119727.
(58) Chen, M.; Li, J. J. Nanofluid-based pulsating heat pipe for thermal management of lithium-ion batteries for electric vehicles. *Journal of Energy Storage* **2020**, *32*, No. 101715.
(59) Ling, Y. Z.; Zhang, X. S.; Wang, F.; She, X. H. Performance study of phase change materials coupled with three dimensional oscillating heat pipes with different structures for electronic cooling. *Renewable Energy* **2020**, *154*, 636−649.
(60) Markal, B.; Varol, R. Thermal investigation and flow pattern analysis of a closed-loop pulsating heat pipe with binary mixtures. *Journal of the Brazilian Society of Mechanical Sciences and Engineering* **2020**, *42*, 549.
(61) Liu, X. D.; Chen, X.; Zhang, Z. W.; Chen, Y. P. Thermal performance of a novel dual-serpentine-channel flat-plate oscillating heat pipe used for multiple heat sources and sinks. *Int. J. Heat Mass Transfer* **2020**, *161*, No. 120293.
(62) Zhou, Z. C.; Lv, Y. J.; Qu, J.; Sun, Q.; Grachev, D. Performance evaluation of hybrid oscillating heat pipe with carbon nanotube nanofluids for electric vehicle battery cooling. *Applied Thermal Engineering* **2021**, *196*, No. 117300.
(63) Kim, J. S.; Bui, N. H.; Kim, J. W.; Kim, J. H.; Jung, H. S. Flow visualization of oscillation characteristics of liquid and vapor flow in the oscillating capillary tube heat pipe. *KSME International Journal* **2003**, *17* (10), 1507−1519.
(64) Jun, S.; Kim, S. J. Comparison of the thermal performances and flow characteristics between closed-loop and closed-end micro pulsating heat pipes. *Int. J. Heat Mass Transfer* **2016**, *95*, 890−901.
(65) Wang, J. S.; Ma, H.; Zhu, Q. Effects of the evaporator and condenser length on the performance of pulsating heat pipes. *Applied Thermal Engineering* **2015**, *91*, 1018−1025.
(66) Lee, J.; Kim, S. J. Effect of channel geometry on the operating limit of micro pulsating heat pipes. *Int. J. Heat Mass Transfer* **2017**, *107*, 204−212.
(67) Hu, Y. X.; Huang, K. X.; Huang, J. A review of boiling heat transfer and heat pipes behavior with self-rewetting fluids. *Int. J. Heat Mass Transfer* **2018**, *121*, 107−118.
(68) Sun, Q.; Qu, J.; Li, X. J.; Yuan, J. P. Experimental investigation of thermo-hydrodynamic behavior in a closed loop oscillating heat pipe. *Experimental Thermal and Fluid Science* **2017**, *82*, 450−458.
(69) Kang, Z. X.; Shou, D. H.; Fan, J. T. Numerical study of a novel Single-loop pulsating heat pipe with separating walls within the flow channel. *Applied Thermal Engineering* **2021**, *196*, No. 117246.
(70) Thompson, S. M.; Ma, H. B.; Wilson, C. Investigation of a flat-plate oscillating heat pipe with Tesla-type check valves. *Experimental Thermal and Fluid Science* **2011**, *35*, 1265−1273.
(71) Liu, J. Y. *A pulsating heat pipe based thermal management system for Lithium-ion batteries*. Ms.Sci. Thesis, Carleton University: Ottawa, 2021.
(72) Tong, B. Y.; Wong, T. N.; Ooi, K. T. Closed-loop pulsating heat pipe. *Applied Thermal Engineering* **2001**, *21*, 1845−1862.

https://doi.org/10.1021/acsomega.3c08056
ACS Omega 2024, 9, 97−116

(73) Xu, J. L.; Li, Y. X.; Wong, T. N. High speed flow visualization of a closed loop pulsating heat pipe. *Int. J. Heat Mass Transfer* **2005**, *48*, 3338−3351.
(74) Senjaya, R.; Inoue, T. Bubble generation in oscillating heat pipe. *Applied Thermal Engineering* **2013**, *60*, 251−255.
(75) Yoon, A.; Kim, S. J. Characteristics of oscillating flow in a micro pulsating heat pipe: Fundamental-mode oscillation. *Int. J. Heat Mass Transfer* **2017**, *109*, 242−253.
(76) Kim, W.; Kim, S. J. Effect of a flow behavior on the thermal performance of closed-loop and closed-end pulsating heat pipes. *Int. J. Heat Mass Transfer* **2020**, *149*, No. 119251.
(77) Perna, R.; Abela, M.; Mameli, M.; Mariotti, A.; Pietrasanta, L.; Marengo, M.; Filippeschi. Flow characterization of a pulsating heat pipe through the wavelet analysis of pressure signals. *Applied Thermal Engineering* **2020**, *171*, No. 115128.
(78) Yoon, I.; Wilson, C.; Borgmeyer, B.; Winholtz, R. A.; Ma, H. B.; Jacobson, D. L.; Hussey, D. S. Neutron phase volumetry and temperature observations in an oscillating heat pipe. *International Journal of Thermal Sciences* **2012**, *60*, 52−60.
(79) Yasuda, Y.; Nabeshima, F.; Horiuchi, K.; Nagai. Visualization of the working fluid in a flat-plate pulsating heat pipe by neutron radiograph. *International Journal of Heat and Mass transfer* **2022**, *185*, No. 122336.
(80) Zhao, J. T.; Wu, C. H.; Rao, Z. H. Numerical study on heat transfer enhancement of closed loop oscillating heat pipe through active incentive method. *International Communications in Heat and Mass Transfer* **2020**, *115*, No. 104612.
(81) Pouryoussefi, S. M.; Zhang, Y. W. Numerical investigation of chaotic flow in a 2D closed-loop pulsating heat pipe. *Applied thermal Engineering* **2016**, *98*, 617−627.
(82) Pouryoussefi, S. M.; Zhang, Y. W. Analysis of chaotic flow in a 2D multi-turn closed-loop pulsating heat pipe. *Applied Thermal Engineering* **2017**, *126*, 1069−1076.
(83) Gernert, N.; Sarraf, D. SteinbergM. Flexible heat pipe cold plates for aircraft thermal control. *SAE Technical Paper* **1991**, No. 912105.
(84) Oshman, C.; Shi, B.; Li, C.; Yang, R. G.; Lee, Y. C.; Peterson, G. P.; Bright, V. M. The development of polymer-based flat heat pipes. *Journal of Micorelectromechanical Systems* **2011**, *20* (2), 410−417.
(85) Oshman, C.; Li, Q.; Liew, L. A.; Yang, R. G.; Lee, Y. C.; Bright, V. M.; Sharar, D. J.; Jankowski, N. R.; Morgan, B. C. Thermal performance of a flat polymer heat pipe heat spreader under high acceleration. *Journal of Micromechanics and Microengineering* **2012**, *22*, No. 045018.
(86) Oshman, C.; Li, Q.; Liew, L. A.; Yang, R. G.; Bright, V. M.; Lee, Y. C. Flat flexible polymer heat pipes. *Journal of Micromechanics and Microengineering* **2013**, *23*, No. 015001.
(87) Hsieh, S. S.; Yang, Y. R. Design, fabrication and performance tests for a polymer-based flexible flat heat pipe. *Energy Conversion and Management* **2013**, *70*, 10−19.
(88) Yang, C.; Chang, C.; Song, C. Y.; Shang, W.; Wu, J. B.; Tao, P.; Deng, T. Fabrication and performance evaluation of flexible heat pipes for potential thermal control of foldable electronics. *Applied Thermal Engineering* **2016**, *95*, 445−453.
(89) Qu, J.; Li, X. J.; Cui, Y. Y.; Wang, Q. Design and experimental study on a hybrid flexible oscillating heat pipe. *Int. J. Heat Mass Transfer* **2017**, *107*, 640−645.
(90) Qu, J.; Wang, C.; Li, X. J.; Wang, H. Heat transfer performance of flexible oscillating heat pipes for electric/hybrid-electric vehicle battery thermal management. *Applied Thermal Engineering* **2018**, *135*, 1−9.
(91) Lim, J. H.; Kim, S. J. Fabrication and experimental evaluation of a polymer-based flexible pulsating heat pipe. *Energy Conversion and Management* **2018**, *156*, 358−364.
(92) Liu, C.; Li, Q.; Fan, D. S. Fabrication and performance evaluation of flexible flat heat pipes for the thermal control of deployable structure. *Int. J. Heat Mass Transfer* **2019**, *144*, No. 118661.
(93) Huang, J. L.; Zhou, W.; Xiang, J. H.; Liu, C. Z.; Gao, Y.; Li, S. L.; Ling, W. S. Development of novel flexible heat pipe with multistage design inspired by structure of human spine. *Applied Thermal Engineering* **2020**, *175*, No. 115392.
(94) Jung, C.; Lim, J.; Kim, S. J. Fabrication and evaluation of a high-performance flexible pulsating heat pipe hermetically sealed with metal. *Int. J. Heat Mass Transfer* **2020**, *149*, No. 119180.
(95) Huang, J. L.; Xiang, J. H.; Chu, X. Y.; Sun, W. J.; Liu, R. L.; Ling, W. S.; Zhou, W.; Tao, S. L. Thermal performance of flexible branch heat pipe. *Applied Thermal Engineering* **2021**, *186*, No. 116532.
(96) Zhao, R.; Gu, J. J.; Liu, J. An experimental study of heat pipe thermal management system with wet cooling method for lithium ion batteries. *Journal of Power Source* **2015**, *273*, 1089−1097.
(97) Liu, F. F.; Lan, F. C.; Chen, J. Q. Dynamic thermal characteristics of heat pipe via segmented thermal resistance model for electric vehicle battery cooling. *J. Power Sources* **2016**, *321*, 57−70.
(98) Liu, F. F.; Lan, F. C.; Chen, J. Q.; Li, Y. G. Experiment investigation on cooling/heating characteristics of ultra-thin micro heat pipe for electric vehicle battery thermal management. *Chinese journal of mechanical engineering* **2018**, *31*, 53.
(99) Ye, X.; Zhao, Y. H.; Quan, Z. H. Thermal management system of lithium-ion battery module base on micro heat pipe array. *International Journal of Energy Research* **2018**, *42*, 648−655.
(100) Ye, X.; Zhao, Y. H.; Quan, Z. H. Experimental study on heat dissipation for lithium-ion battery based on micro heat pipe array (MHPA). *Applied Thermal Engineering* **2018**, *130*, 74−82.
(101) Dan, D.; Yao, C. N.; Zhang, Y. J.; Zhang, H.; Zeng, Z. Z.; Xu, X. M. Dynamic thermal behavior of micro heat pipe array-air cooling battery thermal management system based on thermal network model. *Applied Thermal Engineering* **2019**, *162*, No. 114183.
(102) Mo, X. B.; Hu, X. G.; Tang, J. C.; Tian, H. A comprehensive investigation on thermal management of large-capacity pouch cell using micro heat pipe array. *International Journal of Energy Research* **2019**, *43*, 7444−7458.
(103) Guichet, V.; Khordehgah, N.; Jouhara, H. Experimental investigation and analytical prediction of a multi-channel flat heat pipe thermal performance. *International Journal of Thermofluids* **2020**, *5*−*6*, No. 100038.
(104) Ren, R. Y.; Zhao, Y. H.; Diao, Y. H.; Liang, L.; Jing, H. R. Active air cooling thermal management system based on U-shaped micro heat pipe array for lithium-ion battery. *J. Power Sources* **2021**, *507*, No. 230314.
(105) Liang, L.; Zhao, Y. H.; Diao, Y. H.; Ren, R. Y.; Jing, H. R. Inclined U-shaped flat microheat pipe array configuration for cooling and heating lithium-ion battery modules in electric vehicles. *Energy* **2021**, *235*, No. 121433.
(106) Yue, Q. L.; He, C. X.; Jiang, H. R.; Wu, M. C.; Zhao, T. S. A hybrid battery thermal management system for electric vehicles under dynamic working conditions. *Int. J. Heat Mass Transfer* **2021**, *164*, No. 120528.
(107) Wang, L. C.; Zhao, Y. H.; Quan, Z. H.; Liang, J. N. Investigation of thermal management of lithium-ion battery based on micro heat pipe array. *Journal of Energy Storage* **2021**, *39*, No. 102624.
(108) Liang, L.; Zhao, Y. H.; Diao, Y. H.; Ren, R. Y.; Zhu, T. T.; Li, Y. Experimental investigation of preheating performance of lithium-ion battery modules in electric vehicles enhanced by bending flat micro heat pipe array. *Applied Energy* **2023**, *337*, No. 120896.
(109) Ginting, F. H. S.; Tetuko, A. P.; Asri, N. S.; Nurdiyansah, L. F.; Setiadi, E. A.; Humaidi, S.; Sebayang, P. Surface treatment on metal foam wick of a ferrofluid heat pipe. *Surfaces and Interfaces* **2023**, *36*, No. 102499.

https://doi.org/10.1021/acsomega.3c08056
ACS Omega 2024, 9, 97−116